Title

First-Level Analysis of Heavy Vehicle Simulator Testing on Three RHMA-G Mixes to Investigate Performance with Reclaimed Asphalt Pavement Aggregate Replacement

Authors

Jones, David
Louw, Stephanus

Publication Date

2020-12-01

DOI

10.7922/G2NV9GJ6

December 2020
Technical Memorandum: UCPRC-TM-2020-04

First-Level Analysis of Heavy Vehicle Simulator Testing on Three RHMA-G Mixes to Investigate Performance with Reclaimed Asphalt Pavement Aggregate Replacement

Authors:
D. Jones and S. Louw

California Department of Resources, Recycling and Recovery:
Reclaimed Asphalt Pavement in Rubberized Asphalt Studies

PREPARED FOR:

California Department of Resources, Recycling & Recovery
1001 I St.
Sacramento, CA, 95814

PREPARED BY:

University of California
Pavement Research Center
UC Davis and UC Berkeley

TECHNICAL REPORT DOCUMENTATION PAGE

1. REPORT NUMBER UCPRC-TM-2020-04	2. GOVERNMENT ASSOCIATION NUMBER	3. RECIPIENT'S CATALOG NUMBER
4. TITLE AND SUBTITLE First-Level Analysis of Heavy Vehicle Simulator Testing on Three RHMA-G Mixes to Investigate Performance with Reclaimed Asphalt Pavement Aggregate Replacement		5. REPORT PUBLICATION DATE December 2020 6. PERFORMING ORGANIZATION CODE
7. AUTHOR(S) D. Jones (ORCID 0000-0002-2938-076X) and S. Louw (ORCID 0000-0002-1021-7110)		8. PERFORMING ORGANIZATION REPORT NO. UCPRC-TM-2020-04 UCD-ITS-TM-21-61
9. PERFORMING ORGANIZATION NAME AND ADDRESS University of California Pavement Research Center Department of Civil and Environmental Engineering, UC Davis 1 Shields Avenue Davis, CA 95616		10. WORK UNIT NUMBER 11. CONTRACT OR GRANT NUMBER DRR18128
12. SPONSORING AGENCY AND ADDRESS California Department of Resources, Recycling and Recovery 1001 I St Sacramento, CA 95814		13. TYPE OF REPORT AND PERIOD COVERED Guideline 14. SPONSORING AGENCY CODE
15. SUPPLEMENTAL NOTES DOI: 10.7922/G2NV9GJ6		

16. ABSTRACT

This technical memorandum summarizes a literature review update, elements of the construction of a test track to assess various aspects of gap-graded rubberized asphalt concrete (RHMA-G) mixes with and without the addition of reclaimed asphalt pavement (RAP) as aggregate replacement, and a first-level analysis of the results from the first three Heavy Vehicle Simulator (HVS) tests.

Four different RHMA-G mixes were placed on seven sections on the test track at the UCPRC. Mixes differed by nominal maximum aggregate size (NMAS, 1/2 and 3/4 in.) and the addition of 10% RAP by weight of the aggregate as an aggregate replacement. Single and double lifts of each mix were placed. Apart from the addition of RAP, the mix designs all met current Caltrans specifications. Although Caltrans currently does not permit more than one lift of RHMA-G on projects, the placement of each lift of each mix on the test track met current Caltrans specifications for RHMA-G layers.

The first three HVS tests discussed in this technical memorandum covered the control section (0.2 ft. [60 mm], 1/2 in. NMAS with no RAP), a section with a single lift of 1/2 in. mix with RAP, and a section with two lifts of a 3/4 in. mix with RAP. Results from these first three HVS tests, which focused on rutting performance, indicated the following:

- Performance of all three mixes was satisfactory in terms of the level of trafficking required to reach a terminal average maximum rut of 0.5 in. (12.5 mm).
- The addition of RAP as a coarse aggregate replacement did not appear to have a significant influence on the test results.
- The backcalculated stiffnesses of the RHMA-G layer(s) on each section before and after HVS testing indicate that the trafficking did not cause any significant damage (i.e., loss in stiffness) in any of the three test sections. Stiffnesses increased after trafficking on two of the three sections, which was attributed to a combination of aging and densification of the layers under traffic. Some blending of reclaimed asphalt binder with the asphalt rubber binder over time on these two sections, both containing RAP, may have contributed to this stiffness increase.
- No cracks were observed on any of the sections after trafficking.

Given that only three sections have been tested to date, no recommendations on RHMA-G layer thicknesses or permitting the use of coarse RAP in RHMA-G mixes can be made at this time. These recommendations will be made after all the sections have been tested and the forensic investigations and associated laboratory testing have been completed.

17. KEYWORDS RAP in RHMA, Heavy Vehicle Simulator Testing	18. DISTRIBUTION STATEMENT No restrictions. This document is available to the public through the National Technical Information Service, Springfield, VA 22161	
19. SECURITY CLASSIFICATION (of this report) Unclassified	20. NUMBER OF PAGES 88	21. PRICE None

UCPRC ADDITIONAL INFORMATION

1. DRAFT STAGE Final	2. VERSION NUMBER 1
3. UCPRC STRATEGIC PLAN ELEMENT NUMBER CR-APT	4. CALRECYCLE TASK NUMBER DRR18128
5. CALRECYCLE TECHNICAL LEAD AND REVIEWER(S) N. Gauff	6. FHWA NUMBER N/A

7. PROPOSALS FOR IMPLEMENTATION
None

8. RELATED DOCUMENTS
None

9. LABORATORY ACCREDITATION
The UCPRC laboratory is accredited by AASHTO re:source for the tests listed in this report

10. SIGNATURES

D. Jones **FIRST AUTHOR**	J.T. Harvey **TECHNICAL REVIEW**	D. Spinner **EDITOR**	J.T. Harvey **PRINCIPAL INVESTIGATOR**	N. Gauff **CALRECYCLE TECH. LEAD**	N. Gauff **CALRECYCLE CONTRACT MANAGER**

DISCLAIMER STATEMENT

This document is disseminated in the interest of information exchange. The contents of this report reflect the views of the authors who are responsible for the facts and accuracy of the data presented herein. The contents do not necessarily reflect the official views or policies of the State of California or the Federal Highway Administration. This publication does not constitute a standard, specification, or regulation. This report does not constitute an endorsement by the Department of any product described herein.

PROJECT OBJECTIVES

The ultimate goal of this CalRecycle/Caltrans/UCPRC reclaimed asphalt pavement (RAP) initiative is the development of guidance for determining optimal binder and aggregate replacement rates in rubberized hot mix asphalt (RHMA) mixes containing RAP, without the need for binder extraction, and development of performance-related tests for use in routine mix design and construction quality control and quality assurance. The objective of this part of the research is to conduct Heavy Vehicle Simulator (HVS) tests to better understand performance properties of RHMA mixes containing RAP as an aggregate replacement under heavy traffic loading. This technical memorandum presents the results from the control test section with no RAP and two test sections surfaced with different RHMA-G mixes containing RAP as a coarse aggregate replacement.

ACKNOWLEDGMENTS

The University of California Pavement Research Center acknowledges the following individuals and organizations who contributed to the project:

- Nate Gauff, CalRecycle
- The California Department of Transportation
- Philip Reader, George Reed Construction
- Mike Concanon, Don Matthews, and Marco Estrada, Pavement Recycling Systems
- Kyle Arntson, Albina Asphalt
- Scott Metcalf, Ergon Asphalt
- Mike Selzer, Pacific Northwest Oil
- Fernando Aragon, Aragon Geotechnical
- Anthony Silva, Graniterock Construction
- Nick Schaefer, Surface Systems and Instruments
- Bob Staugaard, Asphalt Pavement and Recycling Technologies (APART)
- The UCPRC Heavy Vehicle Simulator and laboratory operations teams

EXECUTIVE SUMMARY

This technical memorandum summarizes a literature review update, elements of the construction of a test track to assess various aspects of gap-graded rubberized asphalt concrete (RHMA-G) mixes with and without the addition of reclaimed asphalt pavement (RAP) as aggregate replacement, and a first-level analysis of the results from the first three Heavy Vehicle Simulator (HVS) tests.

Apart from the research previously undertaken by the University of California Pavement Research Center (UCPRC) for the California Department of Resources Recycling and Recovery (CalRecycle), only limited published research on the use of RAP in new RHMA mixes was located. The few documents available focused on laboratory testing of dense-graded mixes produced with terminal-blended binders containing completely digested rubber particles smaller than 0.4 mm (passing the #40 sieve). No documented research involving accelerated pavement testing of RHMA mixes containing RAP was located.

Four different RHMA-G mixes were placed on seven sections on the test track at the UCPRC. Mixes differed by nominal maximum aggregate size (NMAS; 1/2 and 3/4 in.) and the addition of 10% RAP by weight of the aggregate as a coarse aggregate replacement. Single and double lifts of each mix were placed. Apart from the addition of RAP, the mix designs all met current Caltrans specifications. Although Caltrans currently does not permit more than one lift of RHMA-G on projects, the placement of each lift of each mix on the test track met current Caltrans specifications for RHMA-G layers.

The first three HVS tests discussed in this technical memorandum covered the control section (0.2 ft. [60 mm], 1/2 in. NMAS with no RAP), a section with a single lift of 1/2 in. NMAS mix with RAP, and a section with two lifts of a 3/4 in. NMAS mix with RAP. Results from these first three HVS tests, which focused on rutting performance, indicated the following:

- Performance of all three mixes was satisfactory in terms of the level of trafficking required to reach a terminal average maximum rut of 0.5 in. (≈12.5 mm).
- The addition of RAP as a coarse aggregate replacement did not appear to have a significant influence on the test results.

- The backcalculated stiffnesses of the RHMA-G layer(s) on each section before and after HVS testing indicate that the trafficking did not cause any significant damage (i.e., loss in stiffness) in any of the three test sections. Stiffnesses increased after trafficking on two of the three sections, which was attributed to a combination of aging and densification of the layers under traffic. Some blending of reclaimed asphalt binder with the asphalt rubber binder over time on these two sections, both containing RAP, may have contributed to this stiffness increase.
- No cracks were observed on any of the sections after trafficking.

Given that only three sections have been tested to date, no recommendations on RHMA-G layer thicknesses or on permitting the use of coarse RAP in RHMA-G mixes can be made at this time. These recommendations will be made after all the sections have been tested and the forensic investigations and associated laboratory testing have been completed.

TABLE OF CONTENTS

LIST OF TABLES

LIST OF FIGURES

LIST OF ABBREVIATIONS

AASHTO	American Association of State Highway and Transportation Officials
Caltrans	California Department of Transportation
CalRecycle	California Department of Resources Recycling and Recovery
CCPR	Cold central plant recycling
ESAL	Equivalent single axle load
FWD	Falling weight deflectometer
HMA	Hot mix asphalt
HVS	Heavy Vehicle Simulator
LVDT	Linear variable differential transformer
MDD	Multi-depth deflectometer
MTD	Maximum theoretical density
NMAS	Nominal maximum aggregate size
PDR	Partial-depth recycling
PPRC	Partnered Pavement Research Center
RAP	Reclaimed asphalt pavement
R-RAP	Rubberized reclaimed asphalt pavement
RHMA	Rubberized hot mix asphalt
RHMA-G	Gap-graded rubberized hot mix asphalt
RHMA-O	Open-graded rubberized hot mix asphalt
RSD	Road surface deflectometer
UCPRC	University of California Pavement Research Center

CONVERSION FACTORS

APPROXIMATE CONVERSIONS TO SI UNITS				
Symbol	**When You Know**	**Multiply By**	**To Find**	**Symbol**
		LENGTH		
in.	inches	25.40	millimeters	mm
ft.	feet	0.3048	meters	m
yd.	yards	0.9144	meters	m
mi.	miles	1.609	kilometers	km
		AREA		
in^2	square inches	645.2	square millimeters	mm^2
ft^2	square feet	0.09290	square meters	m^2
yd^2	square yards	0.8361	square meters	m^2
ac.	acres	0.4047	hectares	ha
mi^2	square miles	2.590	square kilometers	km^2
		VOLUME		
fl. oz.	fluid ounces	29.57	milliliters	mL
gal.	gallons	3.785	liters	L
ft^3	cubic feet	0.02832	cubic meters	m^3
yd^3	cubic yards	0.7646	cubic meters	m^3
		MASS		
oz.	ounces	28.35	grams	g
lb.	pounds	0.4536	kilograms	kg
T	short tons (2000 pounds)	0.9072	metric tons	t
		TEMPERATURE (exact degrees)		
°F	Fahrenheit	(F-32)/1.8	Celsius	°C
		FORCE and PRESSURE or STRESS		
lbf	pound-force	4.448	newtons	N
lbf/in^2	pound-force per square inch	6.895	kilopascals	kPa
APPROXIMATE CONVERSIONS FROM SI UNITS				
Symbol	**When You Know**	**Multiply By**	**To Find**	**Symbol**
		LENGTH		
mm	millimeters	0.03937	inches	in.
m	meters	3.281	feet	ft.
m	meters	1.094	yards	yd.
km	kilometers	0.6214	miles	mi.
		AREA		
mm^2	square millimeters	0.001550	square inches	in^2
m^2	square meters	10.76	square feet	ft^2
m^2	square meters	1.196	square yards	yd^2
ha	hectares	2.471	acres	ac.
km^2	square kilometers	0.3861	square miles	mi^2
		VOLUME		
mL	milliliters	0.03381	fluid ounces	fl. oz.
L	liters	0.2642	gallons	gal.
m^3	cubic meters	35.31	cubic feet	ft^3
m^3	cubic meters	1.308	cubic yards	yd^3
		MASS		
g	grams	0.03527	ounces	oz.
kg	kilograms	2.205	pounds	lb.
t	metric tons	1.102	short tons (2000 pounds)	T
		TEMPERATURE (exact degrees)		
°C	Celsius	1.8C + 32	Fahrenheit	°F
		FORCE and PRESSURE or STRESS		
N	newtons	0.2248	pound-force	lbf
kPa	kilopascals	0.1450	pound-force per square inch	lbf/in^2

*SI is the abbreviation for the International System of Units. Appropriate rounding should be made to comply with Section 4 of ASTM E380. (Revised April 2021)

Blank page

1. INTRODUCTION

1.1 Background to the Study

As asphalt concrete surface layers on highways and airfields reach the end of their design lives, they are being milled off and replaced with new hot mix asphalt (HMA) or new rubberized hot mix asphalt (RHMA). The millings are being added to reclaimed asphalt pavement (RAP) stockpiles, which in turn are reused in new conventional HMA. The amount of RAP used in new conventional HMA in California varies between 15% and 25% by weight of total mix, but this could increase to 40% or higher in the future. Caltrans currently does not permit the use of any RAP in rubberized gap-graded (RHMA-G) mixes or in rubberized open-graded mixes (RHMA-O). However, there is increasing interest in allowing some RAP either as binder or aggregate replacement in RHMA in order to reduce the amount of virgin materials required.

1.2 Completed Research in California

The University of California Pavement Research Center (UCPRC) completed a preliminary study *(1)* for the California Department of Resources Recycling and Recovery (CalRecycle) in 2017 that investigated the potential implications of using reclaimed rubberized asphalt pavement (R-RAP) materials as partial binder and aggregate replacement in new conventional dense-graded HMA mixes and using reclaimed conventional asphalt pavement (RAP) materials as partial binder and aggregate replacement in new RHMA-G mixes.

Limited laboratory test results indicated that adding R-RAP to dense-graded HMA could potentially yield some improvement in overall rutting performance, but it could also have a potentially overall negative effect on fatigue and low-temperature cracking performance. These findings were consistent with those from tests where conventional RAP was used. The degree of change in rutting and cracking resistance in the HMA mixes was dependent on the R-RAP source, with mixes containing millings only from RHMA layers performing slightly better than mixes containing both R-RAP and RAP. These findings did not indicate a reason or justification for separating R-RAP and RAP millings or maintaining separate stockpiles at asphalt plants.

Test results from the RHMA-G mixes containing RAP indicated that rutting performance is likely to improve but that adding RAP could have a potentially overall negative effect on fatigue and low-temperature cracking performance, which would negate the benefits of selecting RHMA-G as an overlay to retard the rate of reflection cracking.

Since only limited testing on asphalt rubber mixes containing RAP was undertaken in this study, further laboratory testing, followed by full-scale field testing in pilot projects or accelerated wheel load testing was recommended on a wider range of virgin binder, virgin aggregate, and RAP material sources to confirm the findings before any changes to current practice are considered.

1.3 Problem Statements Pertinent to Adding RAP to RHMA Mixes

There is growing interest in adding some RAP to RHMA mixes. However, if binder replacement is the goal, then the amount of recycled tire rubber used will be reduced. Binder replacement in HMA mixes is typically achieved by using finer fractions of RAP (i.e., finer than 3/8 in. [9.5 mm]). Research is needed to assess using coarser RAP, left over after removing the finer fractions, in RHMA mixes, focusing on aggregate replacement with minimal binder replacement. This will allow some RAP addition to RHMA-G and potentially RHMA-O mixes, thereby using all processed RAP without reducing the amount of recycled tires that are used.

1.4 Project Objectives

The ultimate goal of this Caltrans/CalRecycle/UCPRC RAP initiative is the development of guidance for determining optimal binder and aggregate replacement rates in RHMA mixes containing RAP, without the need for binder extraction, and development of performance-related tests for use in routine mix design and construction quality control and quality assurance. The objective of this part of the research is to conduct Heavy Vehicle Simulator (HVS) tests to better understand performance properties of RHMA mixes containing RAP under heavy traffic loading. This technical memorandum covers testing on a control section with no RAP and on two test sections surfaced with different RHMA-G mixes containing RAP as an aggregate replacement.

1.5 Measurement Units

Although Caltrans recently returned to the use of US standard measurement units, metric units have always been used by the UCPRC in the design and layout of HVS test tracks, and for laboratory, HVS, and field measurements and data storage. In this report, both US and metric units (provided in parentheses after the US units) are provided in general discussion. In keeping with convention, metric units are used in HVS and laboratory data analyses and reporting, with some US units, where appropriate, to assist the reader. A conversion table is provided on page xiii.

Blank page

2. LITERATURE REVIEW

A literature review of research undertaken on incorporating reclaimed asphalt pavement (RAP) materials in rubberized hot mix asphalt (RHMA), with special focus on accelerated pavement testing, was completed. Research on both RAP binder replacement and RAP aggregate replacement was considered.

Apart from the research previously undertaken by the UCPRC for CalRecycle *(1)*, only limited published research on the use of RAP in new RHMA mixes was located, with most of it focused on laboratory testing of dense-graded mixes produced with terminal-blended binders containing completely digested rubber particles smaller than 0.4 mm (passing the #40 sieve) in size *(2–9)*.

One Canadian study investigated adding 20% RAP (by weight of the mix) into RHMA-G mixes produced with asphalt rubber binder containing 20% rubber by weight of the binder *(10)*. Stiffness, rutting performance, and thermal cracking performance were evaluated. Test results showed that the mixes containing both rubber and RAP performed better than the mixes containing only RAP. The gap-graded mixes were stiffer and performed better in low-temperature cracking tests, while the dense-graded control mix performed better in rutting tests. Mixes containing RAP had lower fracture stress and fracture temperature than the control mixes with conventional binder and the same quantity of RAP, suggesting that rubberized asphalt mixes in general would have better resistance to thermal cracking.

No documented research involving accelerated pavement testing of RHMA mixes containing RAP was located.

Blank page

3. TEST TRACK LOCATION, DESIGN, AND CONSTRUCTION

3.1 Test Track Location

The RHMA-G experiment is located on the North Test Track at the University of California Pavement Research Center facility in Davis, California. An aerial view of the site is shown in Figure 3.1. The track was reconstructed for this project between 01/03/2019 and 05/08/2019. The study described in this report is the fourth research project involving Heavy Vehicle Simulator (HVS) testing undertaken on this test track.

Figure 3.1: Aerial view of the UCPRC research facility.

3.2 Test Track Layout

The North Test Track is 361 ft. (110 m) long and 52.5 ft. (16 m) wide. It has a 2% crossfall in the north-south direction. Four standard-width lanes can be constructed in this space.

The test track layout is shown in Figure 3.2. The gray-shaded area in the figure covers the seven RHMA-G cells tested in this study. The unshaded area covers the three cold central plant recycled (CCPR) materials tested in another parallel study not discussed in this report. All test track measurements and locations discussed in this report are based on this layout.

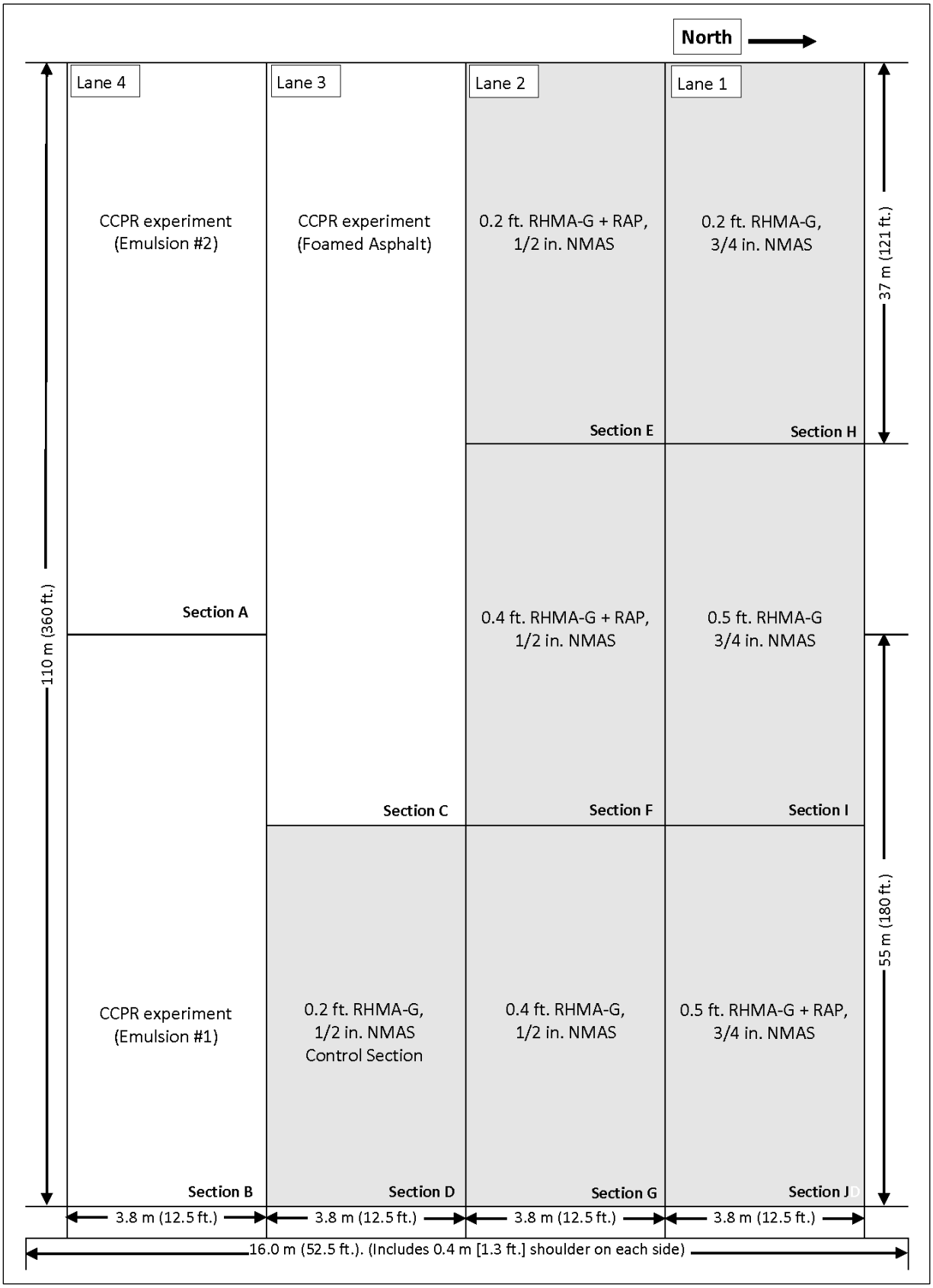

Figure 3.2: Test track layout (shaded area is the RHMA-G experiment).

3.3 Test Track Pavement Design

The pavement design for the test track focused on assessment of both the CCPR layers and the different RHMA-G layers. Given that CCPR layers have not been constructed on the Caltrans road network to date, the test track was designed to be consistent with a typical Caltrans partial-depth recycling (PDR) capital maintenance project to understand the behavior and performance of similar pavement materials recycled using cold central plant technology. A relatively thin (0.2 ft. [60 mm]) RHMA-G surfacing was used in the CCPR material study design and as the control section in the RHMA-G part of the study. A total of four different RHMA-G mixes and two different thicknesses were evaluated in the RHMA-G part of the study. The pavement design for the test track is shown in Figure 3.3 (sections with one RHMA-G layer) and Figure 3.4 (sections with two RHMA-G layers).

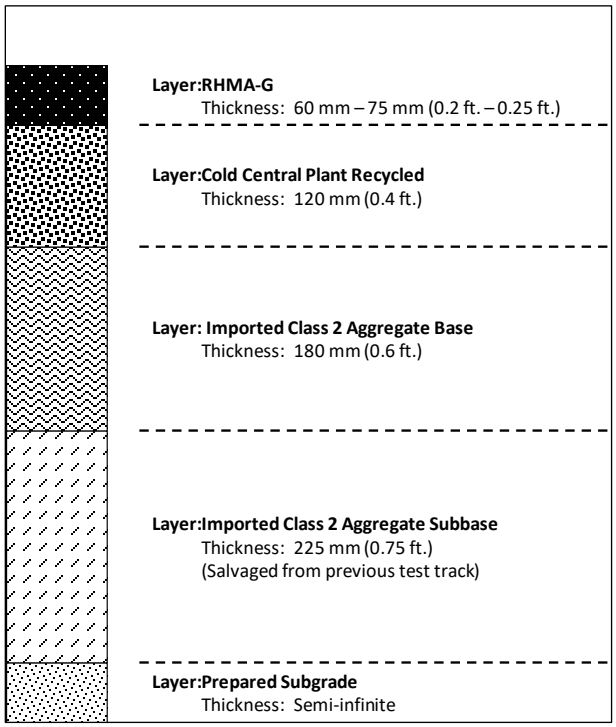

Figure 3.3: Test track design: One RHMA-G layer.

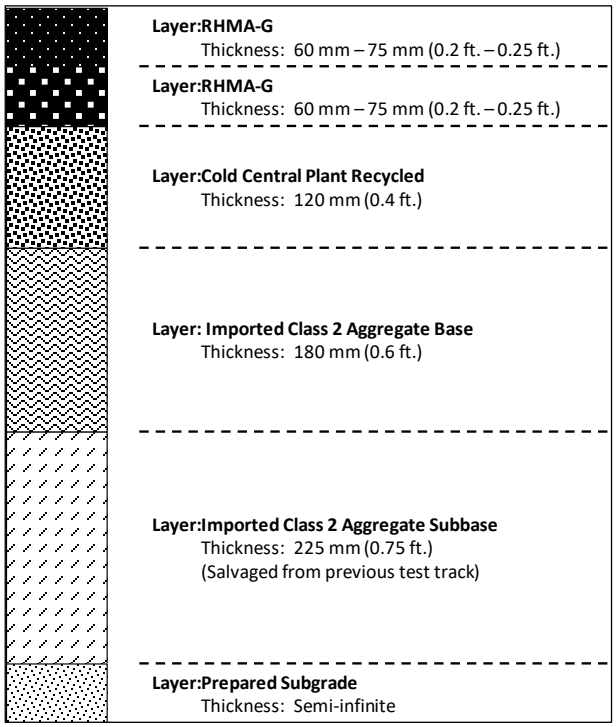

Figure 3.4: Test track design: Two RHMA-G layers.

The different mixes, layer thicknesses, and reasons for inclusion in the study are summarized in Table 3.1.

Table 3.1: Summary of Test Track Sections

Section	RHMA-G Mix	Thickness		Purpose in the Experiment
		(mm)	(ft.)	
D	1/2 in. nominal maximum aggregate size (NMAS), no RAP	60	0.2	Control for all 1/2 in. RHMA-G mixes
E	1/2 in. NMAS with 10% RAP, no binder replacement	60	0.2	Compare mix with RAP to control mix for same layer thickness
F	1/2 in. NMAS with 10% RAP, no binder replacement	120	0.4	Compare two layers, both with RAP, to two layers with no RAP
G	1/2 in. NMAS, no RAP	120	0.4	Compare two layers with single layer
H	3/4 in. NMAS, no RAP	60	0.2	Control for all 3/4 in. RHMA-G mixes. Compare 3/4 in. mix with 1/2 in. mix
I	3/4 in. NMAS, no RAP	150	0.5	Compare two layers with single layer
J	3/4 in. NMAS with 10% RAP, no binder replacement	150	0.5	Compare two layers, both with RAP, to two layers with no RAP

3.4 Test Track Construction

3.4.1 Introduction

Test track reconstruction included the following steps:

1. Removal of the old surfacing layers (asphalt concrete and portland cement concrete).
2. Removal of the old full-depth recycled layers.
3. Removal and temporary stockpiling of the remaining aggregate base layer.
4. Rip and recompact the upper 1 ft. (300 mm) of the subgrade following Caltrans standard specifications. This work was completed on 01/03/2019.
5. Replace the stockpiled old aggregate base materials and shape and compact to form a 0.75 ft. (225 mm) thick aggregate subbase following Caltrans standard specifications. This work was completed on 01/04/2019.
6. Place a new 0.6 ft. (180 mm) thick Class 2 aggregate base following Caltrans standard specifications. This work was completed on 01/23/2019.
7. Apply an emulsified asphalt prime coat to the completed base. This work was completed on 03/14/2019.
8. Produce and place a 0.4 ft. (120 mm) thick layer of cold central plant recycled (CCPR) material. Foamed asphalt (2.5% by weight of the dry aggregate) was used as the recycling agent with 1.0% portland cement active filler. The Caltrans non-standard specification for partial-depth recycling (PDR) was followed for the mix design and placement of the material. This work was completed on 04/24/2019.
9. Apply a fog seal to the CCPR layer. This work was completed on 04/25/2019.
10. Apply a tack coat and place the first lift of RHMA-G mix following Caltrans standard specifications. This work was completed on 05/08/2019.

11. On the applicable sections, apply a tack coat and the second lift of RHMA-G mix following Caltrans standard specifications. This work was completed on 05/08/2019.

The mix design and placement of the RHMA-G layers only is discussed in this report.

3.4.2 RHMA-G Mix Designs

The RHMA-G mixes placed on the test track were designed and produced by George Reed Inc. Key material design parameters from the job mix formulas for the four mixes are summarized in Table 3.2 (no RAP) and Table 3.3 (with RAP). Although Caltrans currently does not allow the use of any RAP materials in RHMA-G mixes, all of the mixes did meet all other Caltrans standard specification requirements for 1/2 in. and 3/4 in. nominal maximum aggregate size (NMAS) RHMA-G mixes.

Table 3.2: Mix Design Parameters for RHMA-G with No RAP

Parameter		1/2 in. NMAS		3/4 in. NMAS	
		Actual	Compliance	Actual	Compliance
Grading (% passing sieve)	1	100	100	100	100
	3/4	100	100	98	95 – 98
	1/2	97	90 – 98	84	83 – 87
	3/8	84	83 – 87	72	65 – 70
	#4	39	28 – 42	36	28 – 42
	#8	19	14 – 22	19	14 – 22
	#200	3.6	0.0 – 6.0	2.7	0.0 – 6.0
RAP content by total weight of aggregate (%)		0	N/A	0	N/A
Base asphalt binder performance grade		64-16	N/A	64-16	N/A
Rubber content (% by weight of binder)		18	18 – 22	18	18 – 22
AR binder cone penetration (mm)		3.6	2.5 – 7.0	3.6	2.5 – 7.0
AR binder resilience (% rebound)		48	> 18	48	> 18
AR binder softening point (°C)		62	52 – 74	62	52 – 74
AR binder viscosity (centipoise)		1,600	1,500 – 4,000	1,600	1,500 – 4,000
Binder content by total weight of mix (%)		7.8	7.4 – 8.3	7.6	7.1 – 8.0
Number of gyrations		150	50 – 150	135	50 – 150
Air-void content (%)		3.8	4.0	4.0	4.0
Voids in mineral aggregate (%)		19.8	18 – 23	19.5	18 – 23
Dust proportion		0.52	N/A	0.44	N/A
Hamburg (rut depth [mm] at 20k passes)		2.2	< 12.5	2.5	< 12.5
Moisture susceptibility, dry strength (psi)		169	> 100	155	> 100
Moisture susceptibility, wet strength (psi)		120	> 70	124	> 70

Table 3.3: Mix Design Parameters for RHMA-G with RAP

Parameter		1/2 in. NMAS		3/4 in. NMAS	
		Actual	Compliance	Actual	Compliance
Grading (% passing sieve)	1	100	100	100	100
	3/4	100	100	97	95 – 98
	1/2	97	90 – 98	83	83 – 87
	3/8	84	83 – 87	72	65 – 70
	#4	41	28 – 42	36	28 – 42
	#8	21	14 – 22	19	14 – 22
	#200	3.4	0.0 – 6.0	2.7	0.0 – 6.0
RAP content by total weight of aggregate (%)		10	N/A	10	N/A
Base asphalt binder performance grade		64-16	N/A	64-16	N/A
Rubber content (% by weight of binder)		18	18 – 22	18	18 – 22
AR binder cone penetration (mm)		3.6	2.5 – 7.0	3.6	2.5 – 7.0
AR binder resilience (% rebound)		48	> 18	48	> 18
AR binder softening point (°C)		62	52 – 74	62	52 – 74
AR binder viscosity (centipoise)		1,600	1,500 – 4,000	1,600	1,500 – 4,000
Binder content by total weight of mix (%)		7.8	7.4 – 8.3	7.75	7.1 – 8.0
Number of gyrations		150	50 – 150	135	50 – 150
Air-void content (%)		4.0	4.0	4.0	4.0
Voids in mineral aggregate (%)		20	18 – 23	19.5	18 – 23
Dust proportion		0.5	N/A	0.43	N/A
Hamburg (rut depth [mm] at 20k passes)		Not tested	< 12.5	Not tested	< 12.5
Moisture susceptibility, dry strength (psi)		Not tested	> 100	Not tested	> 100
Moisture susceptibility, wet strength (psi)		Not tested	> 70	Not tested	> 70

3.4.3 RHMA-G Mix Placement

The RHMA-G mixes were placed on the four lanes of the test track on 05/08/2019. All mixes were produced at the George Reed asphalt plant in Clements, California. Mix was transported in end-dumps, and travel time between the plant and the test track was between 75 and 90 minutes depending on traffic. Production at the plant started at 04:00 hrs. and the first loads departed from the plant at 06:30. The last load was placed at approximately 20:30. Compaction of all sections was completed at approximately 22:00.

Ambient air temperature at 06:30, when activities on the test track started, was 50°F (10°C). Temperatures increased to a high of 85°F (29°C) at 16:00, falling to 65°F (18°C) at 22:00 when compaction on the last section was completed. No clouds were observed during the day. Winds were light, with speeds ranging between 0.3 and 3.0 mph (0.5 and 4.8 km/h) for most of the day, increasing to 6.0 mph (9.6 km/h) in the late afternoon. Relative humidity ranged between a high of 91% at 06:30 and a low of 40% at 16:00, increasing again to 69% at 22:00.

Sections were paved in the following sequence:

1. Section J (3/4 in. with 10% RAP), lift #1
2. Sections I and H (3/4 in. no RAP), lift #1
3. Sections F and E (1/2 in. with 10% RAP), lift #1
4. Sections A, B, C, D, and G (1/2 in. no RAP), lift #1
5. Section G, lift #2
6. Section J, lift #2
7. Section I, lift #2
8. Section F, lift #2

Tack Coat Application

An SS1h tack coat was applied at a rate of 0.03 gal./yd^2 (0.14 L/m^2) approximately 60 minutes prior to placement of the first lift of RHMA-G on each section (Figure 3.5 and Figure 3.6). The tack coat application was repeated prior to placing the second lift of RHMA-G on Sections F, G, I, and J (Figure 3.7).

Figure 3.5: Tack coat application before first lift of RHMA-G (Sections H and I).

Figure 3.6: Close-up view of tack coat application.

Figure 3.7: Tack coat application between lifts of RHMA-G (Section J).

Mix Temperatures

The temperature of the mix in each truckload was measured on arrival when the delivery documentation was checked. Temperatures for the mixes placed on each section are summarized in Table 3.4.

Table 3.4: RHMA-G Temperatures Measured in the Truck

Section	Mix	Lift	Trucks	Time	Temperature	
					°F	°C
J	3/4 in. + 10% RAP	1	2	08:15	333.0	167.2
I and H	3/4 in. no RAP	1	4	09:00 – 09:20	323.9	162.2
F and E	1/2 in. + 10% RAP	1	4	09:30 – 09:50	366.1	185.6
A, B, C, D and G	1/2 in. no RAP	1	10	12:00 – 15:45	330.5	165.8
G	1/2 in. no RAP	2	2	16:10	373.1	189.5
J	3/4 in. + 10% RAP	2	2	18:00	322.2	161.2
I	3/4 in. no RAP	2	2	18:10	349.4	176.4
F	1/2 in. + 10% RAP	2	2	19:50	342.6	172.6

Paving

Paving followed the sequence listed above. Given the confined working space on the test track, the short length of the sections, and small quantities of material required, mix was end-dumped directly into the paver (Figure 3.8) rather than dumping into a windrow and then using a material transfer vehicle to load the paver, as specified in the Caltrans specifications. Thereafter, paving and compaction followed conventional procedures consistent with Caltrans RHMA-G specification requirements (Figure 3.9 through Figure 3.12).

Figure 3.8: Dumping mix into the paver (Section J).

Figure 3.9: Paving first lift of RHMA-G (Section J).

Figure 3.10: Breakdown compaction (Section J).

Figure 3.11: Breakdown (Section G, front) and intermediate compaction (Section J).

Figure 3.12: Final compaction (Sections H and I).

3.5 Construction Quality Control

3.5.1 Temperature

Temperatures were systematically recorded throughout the placement of the RHMA-G using thermocouples (Figure 3.13) and an infrared camera fixed to the paver (Figure 3.14).

Figure 3.13: Temperature measurement with thermocouple.

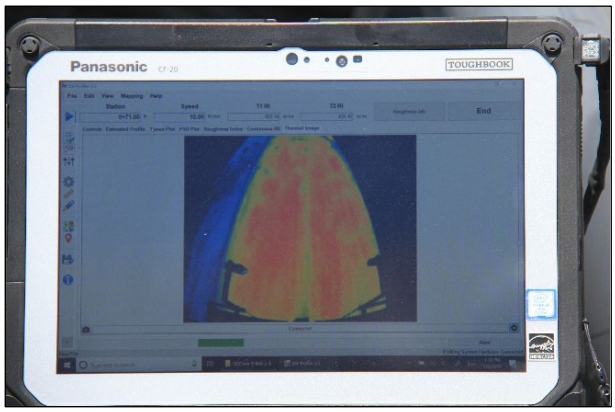

Figure 3.14: Temperature measurement with paver-mounted infrared camera.

Approximate average mix temperatures behind the paver screed and at the start and completion of rolling for each section are summarized in Table 3.5. These temperatures are consistent with typical temperatures on RHMA-G construction projects.

Table 3.5: Approximate Average Mix Temperatures During Construction

Section	Mix	Lift	Average Temperature					
			Behind Paver		Start of Compaction		End of Compaction	
			(°F)	(°C)	(°F)	(°C)	(°F)	(°C)
D	1/2 in. no RAP	1	313	156	304	151	189	87
E	1/2 in. + 10% RAP	1	315	157	295	146	187	86
F	1/2 in. + 10% RAP	1	300	149	280	138	187	86
G	1/2 in. no RAP	1	Not tested					
H	3/4 in. no RAP	1	275	135	309	154	226	108
I	3/4 in. no RAP	1	318	159	288	142	180	82
J	3/4 in. + 10% RAP	1	327	164	259	126	214	101
F	1/2 in. + 10% RAP	2	Not tested					
G	1/2 in. no RAP	2	Not tested					
I	3/4 in. no RAP	2	322	161	255	124	271	133
J	3/4 in. + 10% RAP	2	286	141	277	136	192	89

3.5.2 Compaction Density

Compaction density was measured using a nuclear gauge on the day of construction and on cores removed from each section on the days following construction. Relative compaction was determined using the theoretical specific gravity values (AASHTO T 209) of samples collected behind the paver on each section. Nuclear gauge measurements were taken at three randomly selected locations on each section. A summary of the core density and nuclear gauge density results is provided in Table 3.6. The relative compaction (i.e., percent of maximum theoretical density) achieved on each lift on each section is plotted in Figure 3.15.

The results from cores were used for analysis purposes and indicate that all of the sections had satisfactory compaction and met Caltrans specifications (i.e., 91% to 97% of maximum theoretical density). There was some variability in the measurements across the seven sections, with relative compaction varying between 93.8% and 95.9% with an average of 94.7% and a standard deviation of 2.1%. There were no clear reasons to explain the compaction differences across the seven sections (e.g., mix type, presence of RAP, mix temperature, number of roller passes, etc.) and it was therefore attributed to normal construction variability.

Table 3.6: Summary of RHMA-G Layer Density Measurements

Section	Lift	MTD[1] (g/cm³)	Core Density			Nuclear Gauge Density		
			Average (g/cm³)	Std. Dev.[2] (g/cm³)	Relative (% of MTD)	Average (g/cm³)	Std. Dev. (g/cm³)	Relative (% of MTD)
D	1	2.522	2.378	0.014	94.3	2.299	0.012	91.2
E	1	2.533	2.377	0.029	93.8	2.324	0.020	91.7
F	1	2.533	2.404	0.033	94.9	2.307	0.011	91.1
G	1	2.522	2.373	0.014	94.1	2.324	0.034	92.1
H	1	2.558	2.412	0.044	94.3	2.362	0.056	92.3
I	1	2.558	2.436	0.009	95.2	2.330	0.009	91.1
J	1	2.530	2.390	0.035	94.5	2.382	0.015	94.2
F	2	2.533	2.393	0.016	94.5	2.350	0.027	92.8
G	2	2.522	2.419	0.014	95.9	2.320	0.006	92.0
I	2	2.558	2.436	0.005	95.2	2.357	0.011	92.1
J	2	2.530	2.412	0.035	95.3	2.358	0.019	93.2

[1] MTD = Maximum theoretical density (determined according to AASHTO T 209)
[2] Std. Dev. = Standard deviation

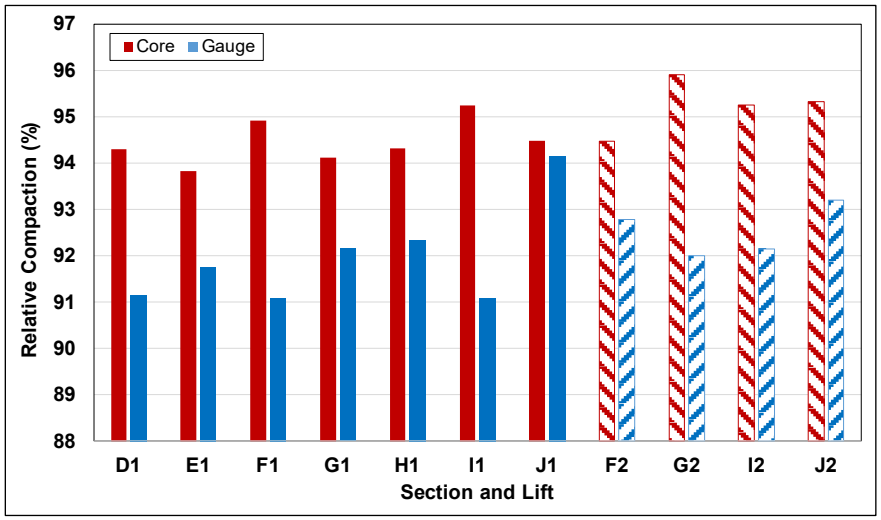

Figure 3.15: Summary of relative density measurements.

3.5.3 As-Built Layer Thicknesses

RHMA-G layer thicknesses were determined from a precise leveling survey with measurements taken every 9.8 ft. (3 m) along the centerline of each lane. Measurements were also recorded from cores cut from the centerline 16.4 ft. (5 m) from the start and end of each section. No cores were taken between these points to ensure that future HVS test sections would not be affected. However, measurements were also taken from the density cores and from cores removed to install the multi-depth deflectometers at Station 13 on each HVS section. The results are summarized in Table 3.7 and indicate that the as-built thicknesses were close to the design thicknesses.

Table 3.7: Layer Thickness Measurements

Section	Mix Type	Design Thickness		Average Thickness		Standard Deviation	
		(ft.)	(mm)	(ft.)	(mm)	(ft.)	(mm)
D	1/2 in. NMAS, no RAP	0.2	60	0.2	65	0.01	3.1
E	1/2 in. NMAS + 10% RAP	0.2	60	0.2	62	0.01	1.6
F	1/2 in. NMAS + 10% RAP	0.4	120	0.4	117	0.01	1.7
G	1/2 in. NMAS + 10% RAP	0.4	120	0.4	119	0.01	2.5
H	3/4 in. NMAS, no RAP	0.2	60	0.2	64	0.01	2.5
I	3/4 in. NMAS, no RAP	0.5	150	0.5	149	0.01	3.2
J	3/4 in. NMAS + 10% RAP	0.5	150	0.5	149	0.01	3.7

4. TRACK LAYOUT, INSTRUMENTATION, AND TEST CRITERIA

4.1 Testing Protocols

The Heavy Vehicle Simulator (HVS) test section layout, test setup, trafficking, and measurements followed standard University of California Pavement Research Center (UCPRC) protocols *(11)*. Details specific to this project are discussed in the following sections.

4.2 Test Track Layout

The test track layout for this project is shown in Figure 4.1. Falling weight deflectometer (FWD) test results were used to identify three uniform HVS test sections in each mix cell, the first for assessing rutting performance under high pavement temperature conditions (Phase 1), and the second and third for potential additional testing (e.g., fatigue cracking performance). Additional testing, if justified, will be identified and motivated based on the results of the first round of testing and associated laboratory testing.

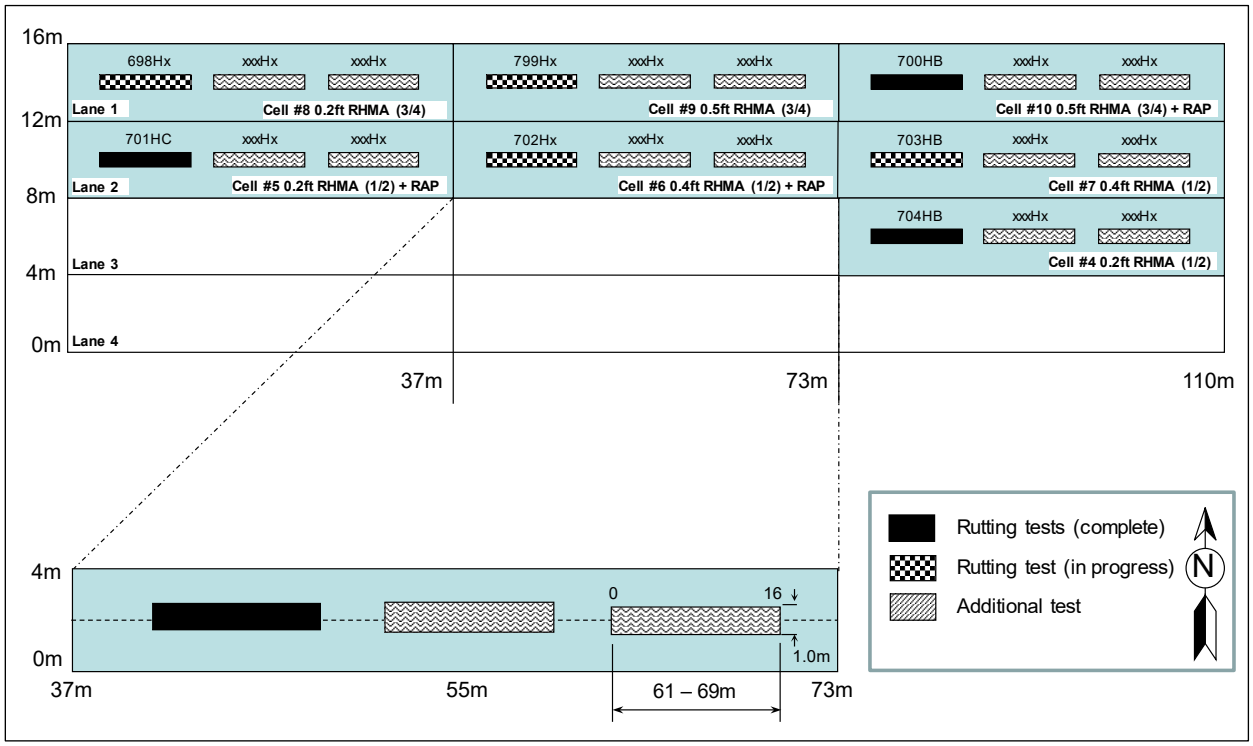

Figure 4.1: Test track layout.

The test section numbers were allocated in order of location on the test track, as follows, and do not represent testing sequence. HB and HC refer to the specific HVS equipment used for testing (x implies that a section number and/or equipment has not been assigned). Section 704HB was considered to be the control section:

- Section 698Hx: 0.2 ft. (60 mm) RHMA-G, with 3/4 in. nominal maximum aggregate size (NMAS) and no RAP
- Section 699Hx: 0.5 ft. (150 mm) RHMA-G, with 3/4 in. NMAS and no RAP
- Section 700HB: 0.5 ft. (150 mm) RHMA-G, with 3/4 in. NMAS with 10% RAP aggregate replacement
- Section 701HC: 0.2 ft. (60 mm) RHMA-G, with 1/2 in. NMAS with 10% RAP aggregate replacement
- Section 702Hx: 0.4 ft. (120 mm) RHMA-G, with 1/2 in. NMAS with 10% RAP aggregate replacement
- Section 703HB: 0.4 ft. (120 mm) RHMA-G, with 1/2 in. NMAS and no RAP
- Section 704HB: 0.2 ft. (60 mm) RHMA-G, with 1/2 in. NMAS and no RAP (Control Section)

This report covers the testing on Sections 700HB, 701HC, and 704HB.

4.3 HVS Test Section Layout

An HVS test section for testing to assess rutting performance is 8.0 m (≈26.2 ft.) long and 0.6 m (≈2 ft.) wide. A schematic in Figure 4.2 shows a typical HVS test section along with the stationing and coordinate system. Station numbers (0 to 16) refer to fixed points on the test section and are used for measurements and as a reference for discussing performance in Chapter 5. Stations are placed at 0.5 m (≈1.6 ft.) increments. A sensor installed at the center of the test section would have an x-coordinate of 4,000 mm and a y-coordinate of 300 mm (≈1.0 ft.).

4.4 Test Section Instrumentation

Measurements were taken with the equipment and instruments listed as follows. Instrument positions are shown in Figure 4.2.

- A laser profilometer was used to measure surface profile; measurements were taken at each station.
- A road surface deflectometer (RSD) was used to measure surface deflection during the test. RSD measurements were taken under a creep-speed 40 kN (9,000 lb.) half-axle load at

regular intervals. Note that RSD measurements under a creep-speed load will not be the same as those recorded under the trafficking speed load. After load changes, deflections were measured under the new load, as well as under the 40 kN load. Only the results from testing under the 40 kN load are discussed in this report. Note that the HVS tests with half an axle. A 40 kN half axle on the HVS equates to an 80 kN (18,000 lb.) full axle on a truck, or one equivalent single axle load (ESAL).

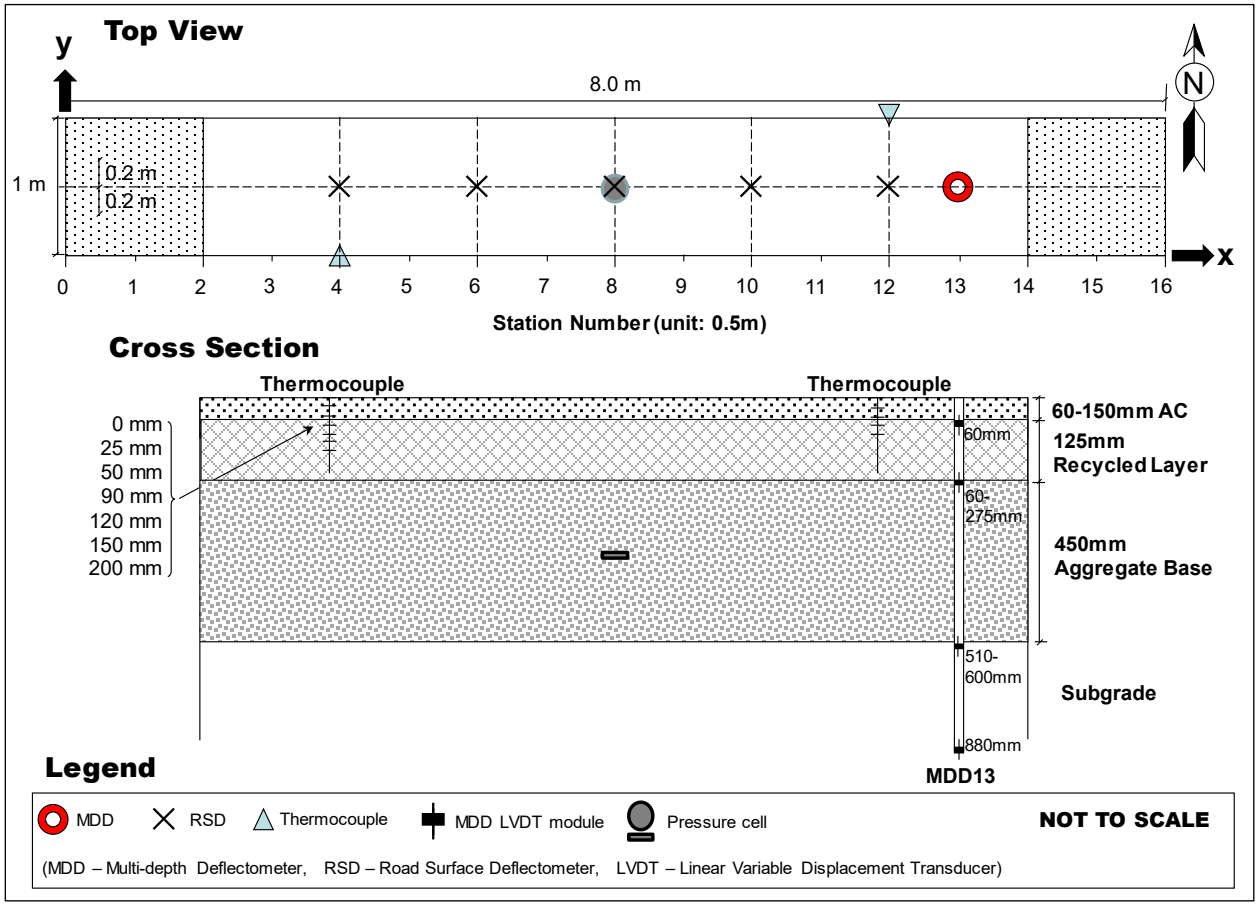

Figure 4.2: Schematic of an HVS test section layout.

- A falling weight deflectometer (FWD) was used to measure surface deflection on the section before and after HVS testing to evaluate the change in stiffness caused by trafficking. Testing was undertaken on both the trafficked and adjacent untrafficked areas (i.e., 5 m on either end of the 8 m test section) at 500 mm (≈19.7 in.) intervals. Two sets of tests were undertaken on each day to obtain a temperature range for backcalculation of layer stiffnesses.
- Type-T thermocouples were used to measure pavement and air temperatures (both inside and outside the HVS environmental chamber). Seven thermocouples were bundled together to form a "thermocouple tree" for measuring air, pavement surface, and

pavement layer temperatures inside the environmental chamber. Pavement layer temperatures were measured at the pavement surface, and at depths of 25, 50, 90, 120, 150, and 200 mm (≈1, 2, 3.5, 4.7, 6, and 8 in.). Air temperatures were measured with thermocouples attached to the outside walls of the environmental chamber, with at least one thermocouple in direct sunlight during any part of the day. Additional air temperatures were recorded at a weather station at the northwest end of the test track.

- One *RST LPTPC09-S* pressure cell was installed at mid-depth in the aggregate base layer (Figure 4.3) on each Phase 1 test section to measure vertical pressure (stress) under the moving wheel.

Figure 4.3: Pressure cell installation.

- One multi-depth deflectometer (MDD) was installed on each Phase 1 test section. An MDD is essentially a stack of linear variable differential transformer (LVDT) modules fixed at different depths in a single borehole. The LVDT modules have non-spring-loaded core slugs that are linked together into one long rod that is anchored at the bottom of a 3.3 m (≈10.8 ft.) borehole. The LVDT modules are fixed to the pavement layer, which allows permanent vertical deformations at various depths to be recorded, in addition to measurement of the elastic deformation caused by the passage of the HVS wheels. The borehole is 38 mm (≈1.5 in.) in diameter. A model MDD with five modules is shown in Figure 4.4. In this project, MDDs were installed between the two wheelpaths of the dual-wheel configuration because of cable limitations that prevented installation in one of the wheelpaths.

Figure 4.4: A model multi-depth deflectometer (MDD), showing five modules.

4.5 Test Section Measurements

4.5.1 Temperature

Pavement temperatures were controlled using an environmental chamber. Both air (inside and outside the environmental chamber) and pavement temperatures were monitored and recorded hourly during the entire trafficking period. In assessing rutting performance, the temperature at the bottom of the asphalt concrete and the temperature gradient from top to bottom of the asphalt concrete layers are two important controlling temperature parameters that influence the stiffness of the asphalt concrete and are used to compute plastic strain.

4.5.2 Surface Profile

The following rut parameters were determined from laser profilometer measurements:

- Maximum total rut depth at each station
- Average maximum total rut depth for all stations
- Average deformation for all stations
- Location and magnitude of the maximum rut depth for the section
- Rate of rut development over the duration of the test

The difference between the surface profile after HVS trafficking and the initial surface profile before HVS trafficking is the permanent change in surface profile. Based on the change in surface profile, the maximum total rut is determined for each station, as illustrated in Figure 4.5. The average maximum total rut for the section is the average of all of the maximum total ruts measured between Stations 3 and 13.

4.5.3 Pressure (Vertical Strain)

Example data recorded from one of the pressure cells is shown in Figure 4.6, which shows the variation of the strain gauge reading versus wheel position as the wheel travels from one end of the test section to the other. Several quantities are summarized based on the raw readings. Specifically, the reference value is the reading when the wheel is at the far end of the test section. The peak and valley are maximum and minimum values deviating from the reference value, respectively.

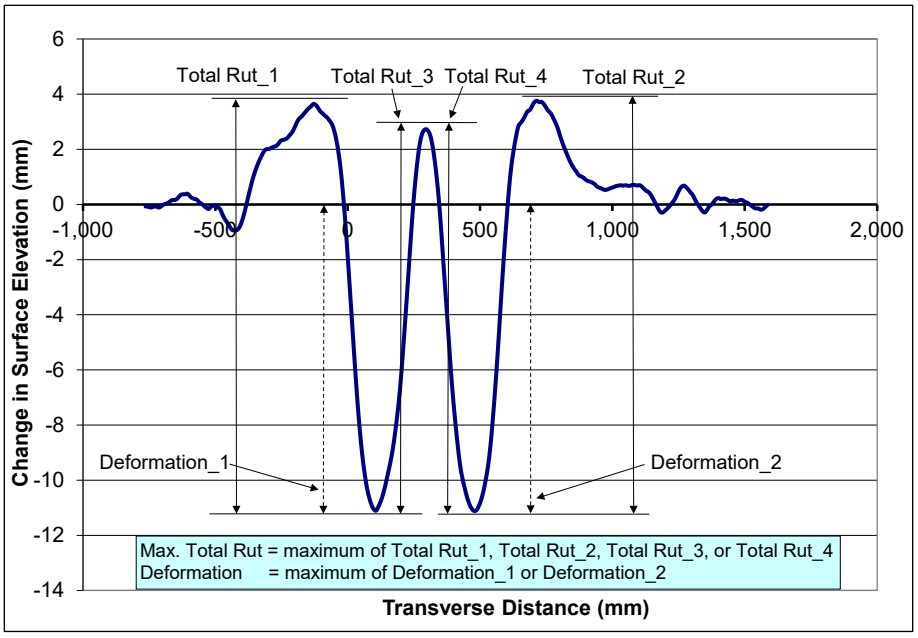

Figure 4.5: Illustration of maximum rut depth and deformation for a leveled profile.

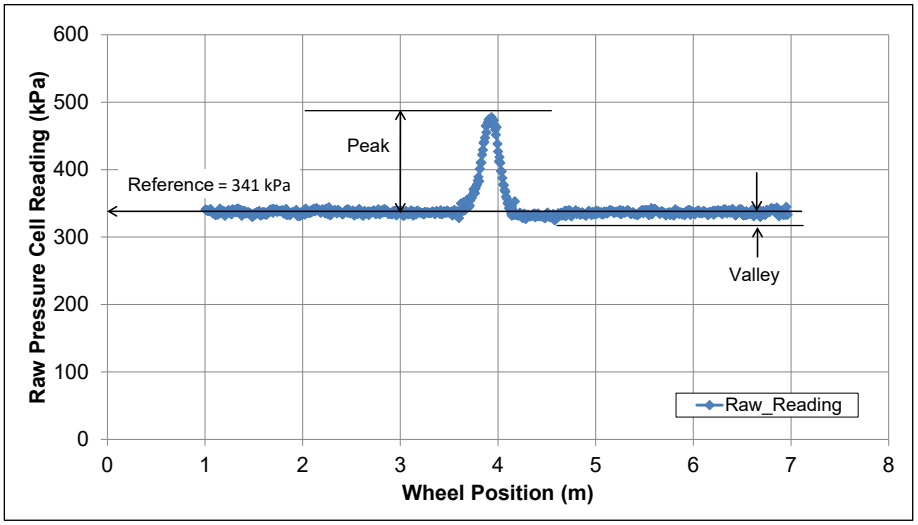

Figure 4.6: Example pressure cell reading and definition of summary quantities.

4.5.4 Elastic Vertical Deflection

An example set of MDD data is presented in Figure 4.7, which shows the variation of the elastic vertical deflections measured at different depths versus wheel position as the wheel travels from one end of the test section to the other. The elastic vertical deflection is the difference between the total vertical deflection and the reference value, which is the measurement recorded when the wheel is at the far end of the test section. The peak values are the maximum elastic vertical deflection for each individual MDD module.

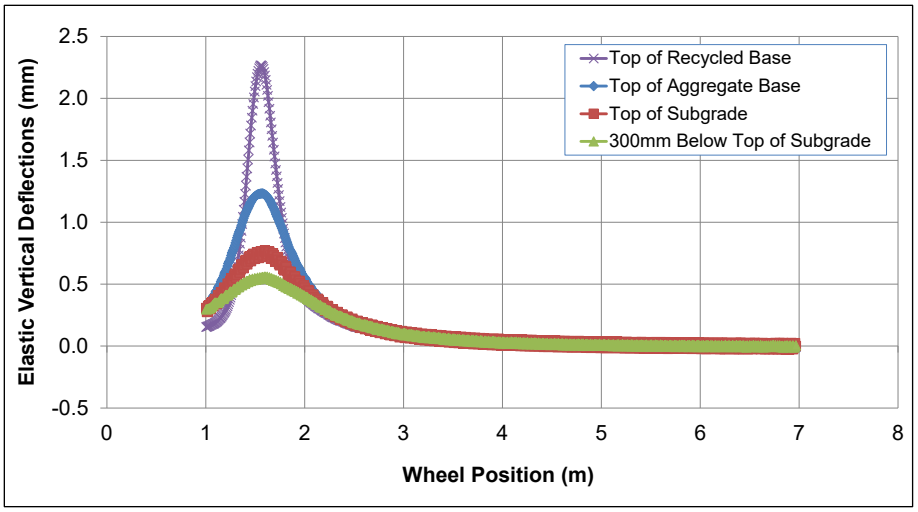

Figure 4.7: Example elastic vertical deflection measured with MDD.

4.6 HVS Test Criteria

4.6.1 Test Section Failure Criteria

An average maximum rut depth of 12.5 mm (≈0.5 in.) and/or an average crack density of 2.5 m/m^2 (≈0.75 ft./ft^2) over the full monitored section (Station 3 to Station 13) were set as the failure criteria for the experiment. In some instances, HVS trafficking was continued past these points so the rutting and/or cracking behavior of a test section could be fully understood.

4.6.2 Environmental Conditions

Infrared heaters and a chilling unit installed inside the HVS environmental chamber were used to maintain pavement temperatures. All sections were tested predominantly during dry conditions, with small amounts of infrequent rainfall recorded during two of the three tests (700HB and 701HC). Only two significant rainfall events (i.e., more than 25 mm [≈1.0 in.] in 24 hours for this study) occurred. The test sections received no direct rainfall as they were protected by the environmental chamber.

The pavement temperature at 50 mm (≈2.0 in.) pavement depth was maintained at 50±2°C (≈122±4°F) to assess rutting performance in the RHMA-G layers under hot pavement conditions.

4.6.3 Test Duration

HVS trafficking on each section was initiated and completed, as shown in Table 4.1. The sequence of testing was adjusted to accommodate positioning of the two HVS machines on the test

sections (i.e., the machines cannot test side by side on the test track configuration because of space limitations). Note that significant delays in testing were experienced due to COVID-19 mandated shutdowns, which also led to delays in receiving critical parts for equipment maintenance and repairs.

Table 4.1: HVS Test Duration

Section No.	Layer Properties	Test Sequence	Start Date	Finish Date	Load Repetitions
700HB	0.5 ft. RHMA-G (3/4 in.) + RAP	1	08/09/2019	11/27/2019	600,000
701HC[1]	0.2 ft. RHMA-G (1/2 in.) + RAP	2	09/06/2019	07/23/2020	300,000
704HB	0.2 ft. RHMA-G (1/2 in.)	3	07/05/2020	09/16/2020	320,000

[1] 701HC was tested in two phases (09/09/2019 to 11/25/2019 and then 06/17/2020 to 07/23/2020) due to an equipment breakdown followed by mandated COVID-19 shutdowns.

4.6.4 HVS Loading Program

The HVS loading program for each section in each testing phase is summarized in Table 4.2. Equivalent single axle loads (ESALs) were determined using the following Caltrans conversion (Equation 4.1):

$$ESALs = (\text{axle load}/18{,}000)^{4.2} \quad \textbf{(4.1)}$$

Table 4.2: Summary of HVS Loading Program

Section No.	Layer Properties	Wheel Load[1] (kN)	Load Repetitions	ESALs[2]	Test to Failure?
700HB	0.5 ft. RHMA-G (3/4 in.) + RAP	40	160,000	160,000	Yes (Rut depth)
		60	100,000	549,014	
		80	340,000	6,248,919	
		Section Total	600,000	6,957,933	
701HC	0.2 ft. RHMA-G (1/2 in.) + RAP	40	160,000	160,000	Yes (Rut depth)
		60	100,000	549,014	
		80	40,000	735,167	
		Section Total	300,000	1,444,181	
704HB	0.2 ft. RHMA-G (1/2 in.) Control	40	160,000	160,000	Yes (Rut depth)
		60	100,000	549,014	
		80	60,000	1,102,750	
		Section Total	320,000	1,811,764	
		Total for the Three Sections	1,220,000	10,213,878	

[1] 40 kN = 9,000 lb.; 60 kN = 13,5000 lb.; 80 kN = 18,000 half-axle loads

[2] ESAL: Equivalent single axle load

All trafficking was carried out with a dual-wheel configuration, using radial truck tires (Goodyear G159 - 11R22.5- steel belt radial) inflated to a pressure of 720 kPa (104 psi), in a channelized, unidirectional loading mode with no wander (i.e., trafficking in one direction consistent with

standard procedures for testing asphalt concrete layer performance). Load was checked with a portable weigh-in-motion pad at the beginning of each test.

Blank page

5. PHASE 1A HVS TEST DATA SUMMARY

5.1 Introduction

This phase of HVS testing was carried out to compare performance of three different RHMA-G mixes. Pavement temperature at 50 mm (≈2.0 in.) pavement depth was maintained at 50±2°C (≈122±4°F) to assess primarily rutting but also cracking potential in the RHMA-G surfacing layer(s). This temperature is consistent with similar HVS testing in past projects. This chapter provides a summary of the data collected from the three Phase 1a HVS tests (Sections 700HB, 701HC, and 704HB) and a brief discussion of the first-level analysis. The following data were collected:

- Rainfall
- Air temperatures outside and inside the environmental chamber
- Pavement temperatures at the surface and 25, 50, 90, 120, 150, and 200 mm below the surface
- Surface permanent deformation (rutting)
- Permanent deformation at the top of the recycled layer, top of the aggregate base layer, top of the original subbase layer, top of the subgrade, and approximately 300 mm below the top of the subgrade
- Pressure (vertical stress) in the middle of the recycled layer
- Elastic vertical deflection at the top of the recycled layer, top of the aggregate base layer, top of the original subbase layer, top of the subgrade, and approximately 300 mm below the top of the subgrade
- Pavement deflection and layer stiffnesses

Note that, where possible, x and y axis scales in graphs have been kept the same for the three tests to facilitate visual comparison of the results.

5.2 Rainfall

Figure 5.1 shows the monthly rainfall data from July 1, 2019, through October 31, 2020, as measured at the weather station next to the test track. Some rainfall was recorded during testing on 700HB and 701HC, with five 24-hour rainfall events greater than 12.5 mm (≈0.5 in.), two of which were greater than 25 mm (≈1 in.). No rainfall was recorded during testing on 704HB.

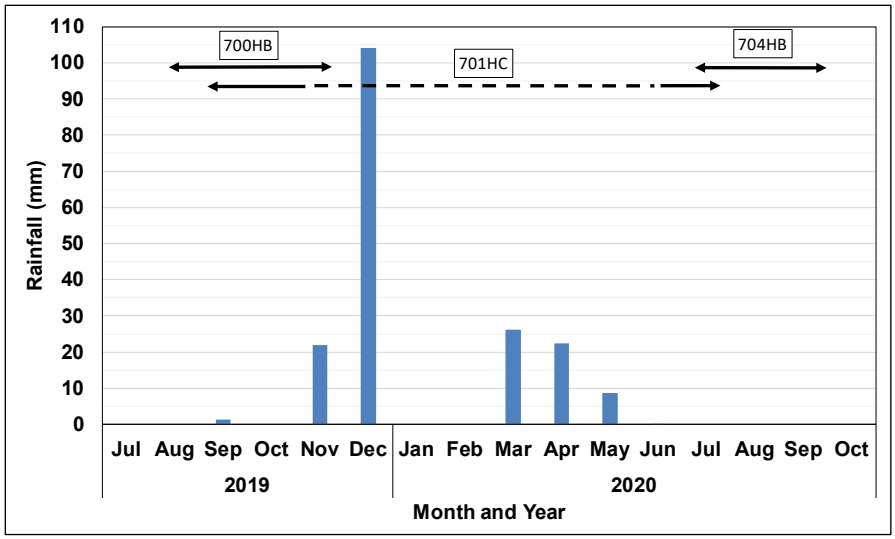

Figure 5.1: Measured rainfall during Phase 1a HVS testing.

5.3 Section 704HB: 0.2 ft. RHMA-G (1/2 in.) Control Section

5.3.1 Test Summary

Loading commenced with a 40 kN half-axle load on July 6, 2020, and ended with an 80 kN load on September 18, 2020. A total of 320,000 load repetitions were applied and 36 datasets were collected. Load was increased from 40 kN to 60 kN after 160,000 load repetitions, and then to 80 kN after 260,000 load repetitions. The HVS loading history for Section 704HB is shown in Figure 5.2. A 21-day breakdown resulting from a hydraulic system failure occurred between August 6 and August 26.

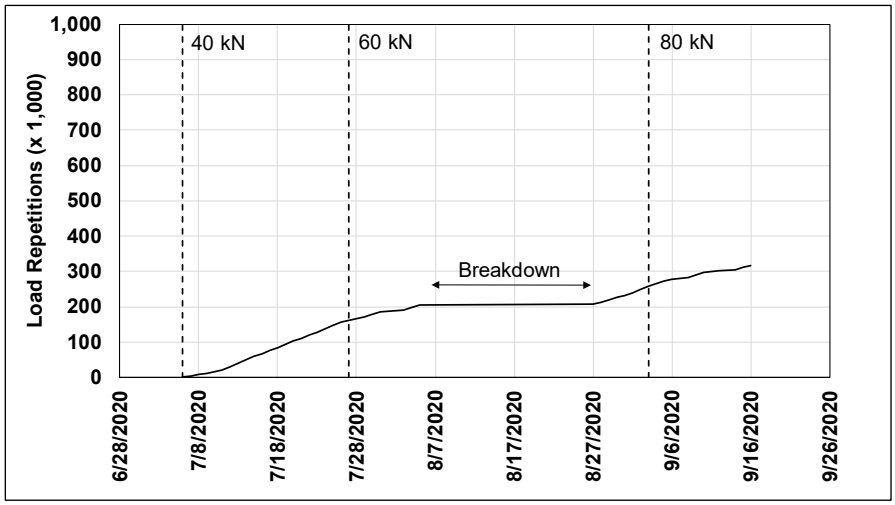

Figure 5.2: 704HB: HVS loading history.

5.3.2 Air Temperatures

Outside Air Temperatures

Daily 24-hour average outside air temperatures, measured with thermocouples attached to either side of the HVS environmental chamber (i.e., in direct sunlight), are summarized in Figure 5.3. Vertical error bars on each point on the graph show the daily temperature range. Temperatures ranged from 13.4°C to 52.9°C (≈56°F to 127°F) during the course of HVS testing, with a daily 24-hour average of 27.2°C (≈81°F), an average minimum of 19.2°C (≈67°F), and an average maximum of 40.4°C (≈104°F).

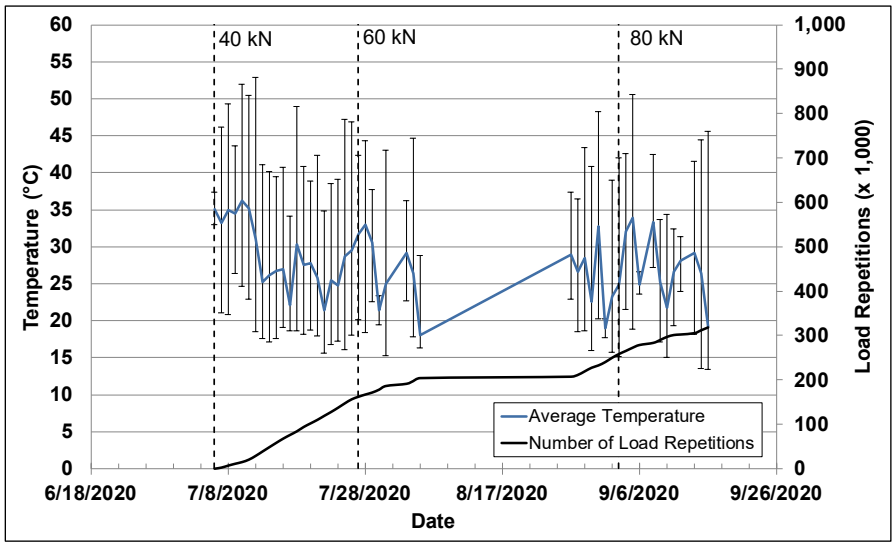

Figure 5.3: 704HB: Daily average air temperatures outside the environmental chamber.

Air Temperatures Inside the Environmental Chamber

The daily 24-hour average air temperatures, measured with thermocouples attached to either side of the HVS environmental chamber above the heaters, calculated from the hourly temperatures recorded during HVS operations, are shown in Figure 5.4. Vertical error bars on each point on the graph show the daily temperature range. During the test, air temperatures inside the environmental chamber ranged from 21.9°C to 51.2°C (≈71°F to 124°F) with an average of 42.8°C (≈109°F) and a standard deviation of 2.9°C (≈5.1°F). Heaters were automatically adjusted to maintain a pavement temperature of 50±2°C at a pavement depth of 50 mm. The recorded pavement temperatures discussed in Section 5.3.3 indicate that the inside air temperatures were adjusted appropriately to maintain the required pavement temperature.

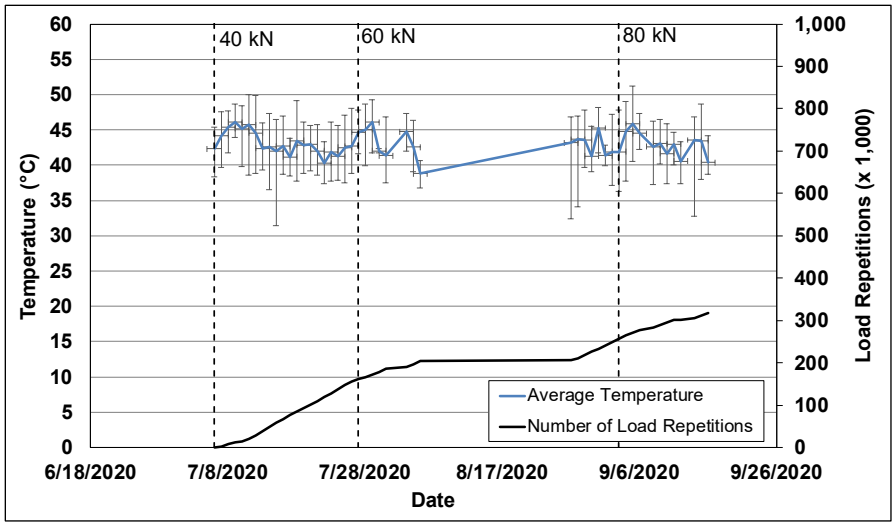

Figure 5.4: 704HB: Daily average air temperatures inside the environmental chamber.

5.3.3 Pavement Temperatures

Daily 24-hour averages of the air, surface, and in-depth temperatures of the RHMA-G and recycled layers are shown in Figure 5.5 and listed in Table 5.1. Pavement temperatures were constant and in the target range (50±2°C at a pavement depth of 50 mm) in the RHMA-G layer. Temperatures decreased with increasing depth in the underlying layers, as expected.

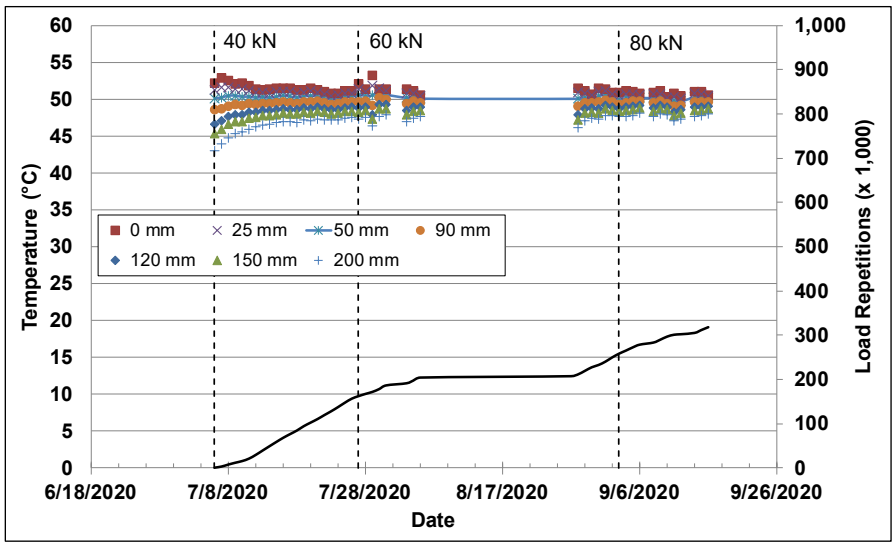

Figure 5.5: 704HB: Daily average pavement temperatures.

Table 5.1: 704HB: Summary of Air and Pavement Temperatures

Thermocouple Location	Layer	Temperature			
		Average (°C)	Std. Dev. (°C)	Average (°F)	Std. Dev. (°F)
Outside air	N/A	27.2	8.5	80.9	15.3
Inside air	N/A	42.8	2.9	109.0	5.1
Pavement surface	RHMA-G	51.2	1.7	124.2	3.1
25 mm below surface	RHMA-G	50.9	0.9	123.5	1.6
50 mm below surface	RHMA-G	50.3	0.6	122.5	1.2
90 mm below surface	Recycled	49.5	0.6	121.1	1.1
120 mm below surface	Recycled	48.7	0.6	119.6	1.1
150 mm below surface	Recycled	48.1	0.7	118.6	1.3
200 mm below surface	Aggregate base	47.1	0.9	116.8	1.6

5.3.4 Permanent Deformation on the Surface (Rutting)

Figure 5.6 shows the average transverse cross section measured with the laser profilometer at various stages of the test. This plot clearly shows the initial high rate of rutting and the increase in rutting and deformation over time and that most of the deformation was in the form of a depression (i.e., deformation was below the zero elevation point at the surface [see Figure 4.5]) rather than upward and outward displacement of the material above the zero elevation point.

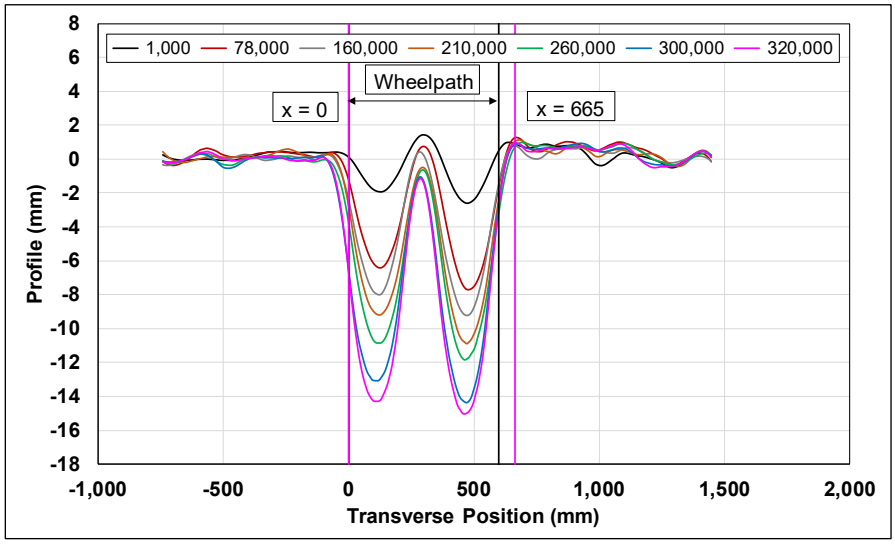

Figure 5.6: 704HB: Profilometer cross section at various load repetitions.

Figure 5.7 shows the development of permanent deformation (average maximum total rut and average deformation) with load repetitions. Error bars on the plot indicate lowest and highest measurement along the section. These error bars show that there was considerable variation in rut depth along the length of the section. The cause of this variation cannot be determined from

the data alone and will be investigated during the forensic investigation upon completion of all testing and as part the laboratory testing phase.

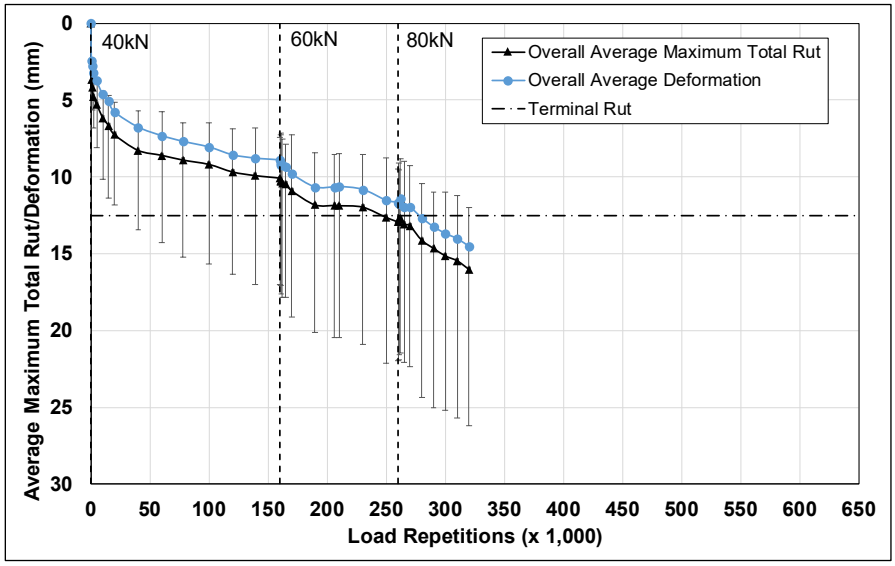

Figure 5.7: 704HB: Average maximum total rut and average deformation.

During HVS testing, rutting usually occurs at a high rate initially and then typically diminishes as trafficking progresses until reaching a steady state. This initial phase is referred to as the "embedment" phase. The embedment phase in this test, although relatively short in terms of the number of load repetitions (i.e., ±20,000), ended with a fairly significant early rut of about 7 mm (≈0.28 in.). Construction data did not provide any clear reason for this behavior. The rate of increase of the rut depth after the embedment phase slowed considerably. The increase in the applied load to 60 kN resulted in a short embedment phase, before stabilizing to a similar rate recorded during the 40 kN testing. After the load increase to 80 kN, the rate of rut depth increased and did not change significantly until the end of the test.

Figure 5.8 shows the average deformation and the deformation measured between Stations 3 and 7 and between Stations 8 and 13. It is clear that deformation was more severe between Stations 8 and 13, which would have influenced the variability discussed previously.

Figure 5.9 and Figure 5.10 show contour plots of the pavement surface at the start and end of the test (320,000 load repetitions). The end-of-test plot clearly shows the deeper rut at one end of the section.

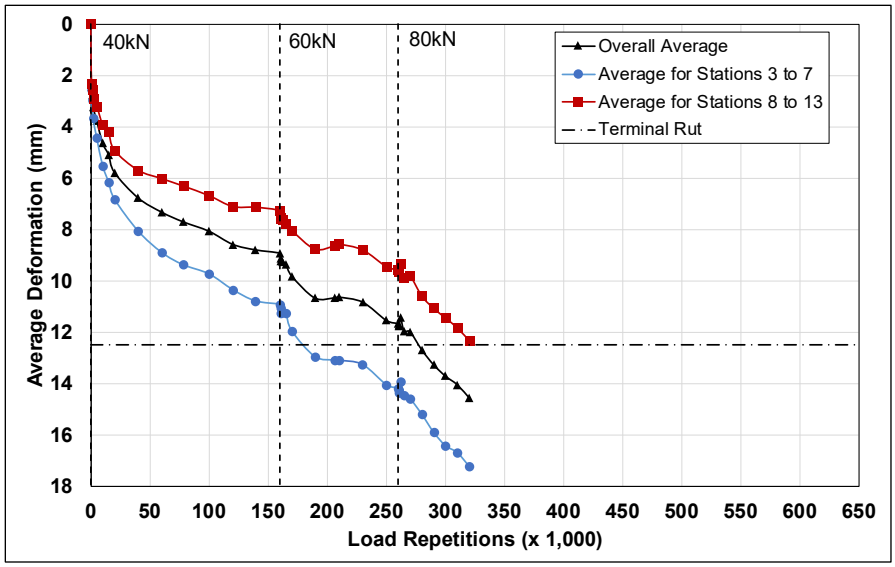

Figure 5.8: 704HB: Average deformation.

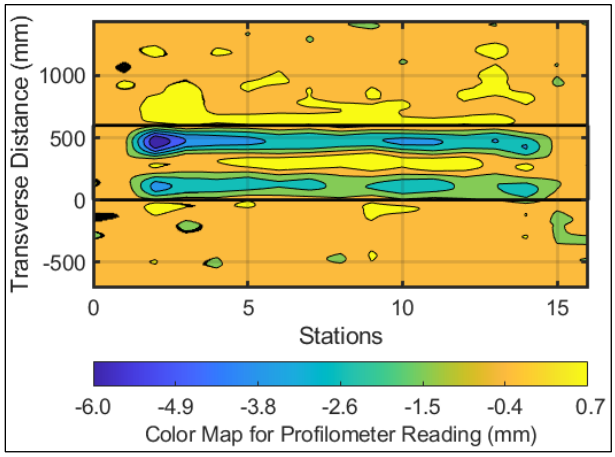

Figure 5.9: 704HB: Contour plot of permanent surface deformation at start of test.

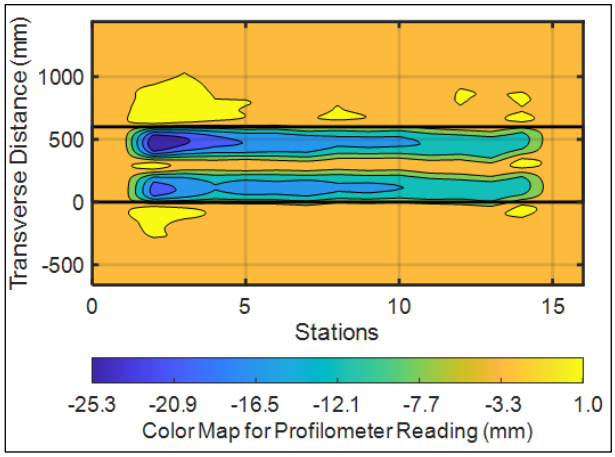

Figure 5.10: 704HB: Contour plot of permanent surface deformation at end of test.
(Note different scales in the legends.)

Terminal rut (12.5 mm [≈0.5 in.]) was reached after approximately 260,000 load repetitions (≈710,000 ESALs). However, since the average maximum rut is calculated from measurements at Stations 3 through 13, and the deeper rut at one end of the section influenced this average, trafficking was continued for another 60,000 additional load repetitions to further assess rutting trends at the 80 kN load.

After completion of trafficking, the average maximum rut depth and the average deformation were 16.0 mm (≈0.63 in.) and 14.6 mm (≈0.57 in.), respectively. The maximum rut depth measured on the section was 21.7 mm (≈0.85 in.), recorded at Station 3.

5.3.5 Permanent Deformation in the Underlying Layers

Permanent deformation in the underlying layers, recorded with a multi-depth deflectometer (MDD) at Station 13 and compared to the surface layer (laser profilometer deformation [not total rut] measurement at Station 13), is shown in Figure 5.11. The LVDT positioned in the CCPR layer failed early in the test and could not be replaced. Note that the MDD measurements only provide an approximate indication of deformation in the underlying layers because the MDD was installed in the untrafficked area between the wheelpaths. This instrument location can therefore only provide an indication of which layer or layers the permanent deformation occurred in and not the actual deformation in each layer, which will be assessed during forensic investigations when all testing is completed.

Figure 5.11 shows that permanent deformation likely occurred predominantly in the RHMA-G, CCPR, and aggregate base layers. The absence of data from the damaged LVDT in the CCPR layer limits any further interpretation of the plot. However, the plot clearly shows minimal permanent deformation in the aggregate subbase and subgrade. Load changes did not appear to have had a significant effect on permanent deformation in the aggregate subbase and subgrade.

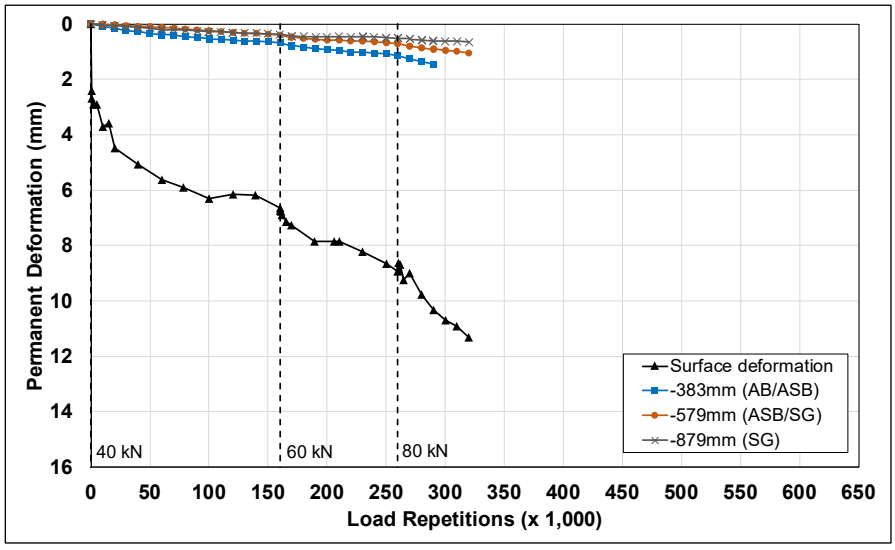

Figure 5.11: 704HB: Permanent deformation in the underlying layers.

5.3.6 Vertical Pressure at the Midpoint of the Aggregate Base Layer

Figure 5.12 shows the traffic-induced vertical pressure in the middle of the aggregate base layer. Note that vertical pressure measurements are recorded continuously during trafficking and

spikes in the measurements indicate when manual measurements, which are done at creep wheel speed, were taken.

Pressure readings were stable after some initial embedment, but sensitive to load change, for the duration of the test. Increases in recorded pressures occurred after the load changes, as expected.

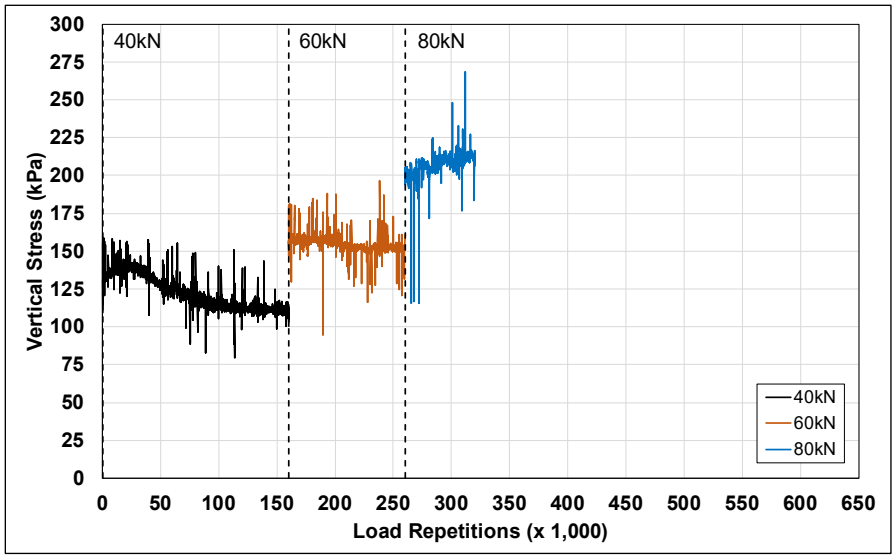

Figure 5.12: 704HB: Vertical pressure in the middle of the aggregate base layer.

5.3.7 Deflection on the Surface (Road Surface Deflectometer)

Figure 5.13 compares elastic surface deflections measured with a road surface deflectometer (RSD) under a 40 kN half-axle load. Deflections under the 60 kN and 80 kN half-axle loads are also shown. Error bars on the 40 kN load measurements indicate lowest and highest measurements along the section for that load. Deflections increased during the embedment phase of each load, as expected, but appeared to stabilize after embedment under the 40 kN and 60 kN loads, indicating that no significant permanent damage occurred in the pavement for the duration of this part of the testing. After the 80 kN load change, deflections under a 40 kN load continued to increase slowly, indicating that some permanent damage was occurring in the pavement under the higher load at the time when testing was halted. Increases in absolute surface deflection were recorded on the section under the 60 kN and 80 kN loads, as expected. The error bars show that there was limited variability in stiffness along the section.

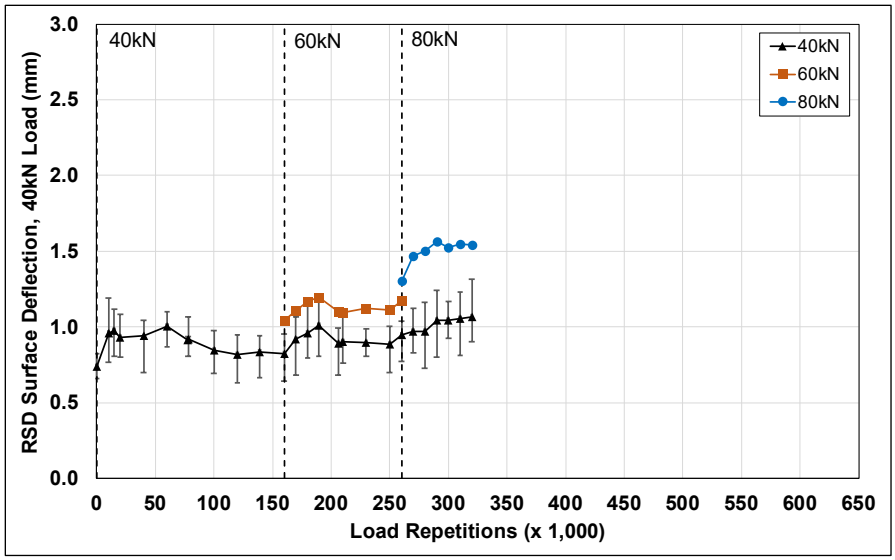

Figure 5.13: 704HB: Surface deflection (RSD).

5.3.8 Deflection in the Underlying Layers (Multi-Depth Deflectometer)

Figure 5.14 shows the history of in-depth elastic deflections measured by the LVDTs in the multi-depth deflectometer. These readings are consistent with the surface deflections measured with the RSD shown in Figure 5.13. Deflections remained stable for the duration of testing under a 40 kN wheel load.

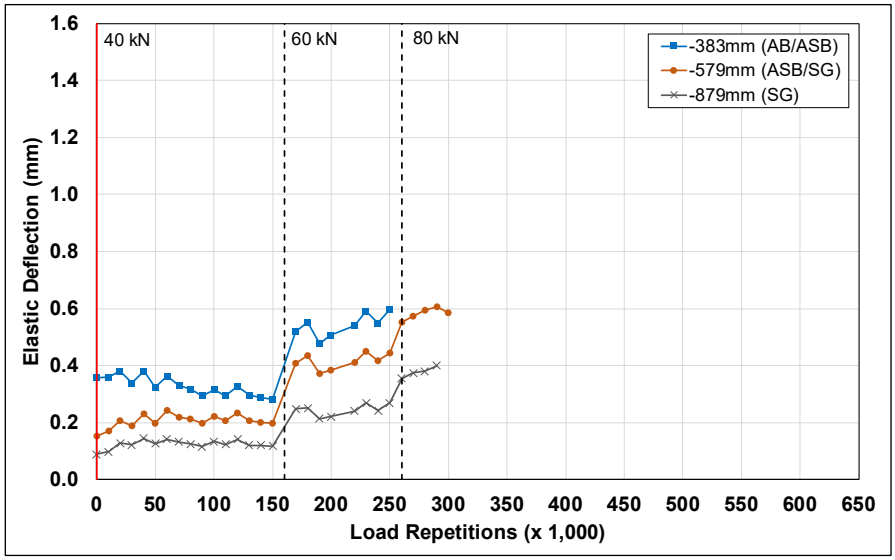

Figure 5.14: 704HB: Elastic deflection in the underlying layers.

Deflections increased with increased load, as expected, and continued to slowly increase during trafficking, indicating that only minimal damage was occurring under the heavier wheel loads.

Deflection decreased with increasing depth, but the LVDTs at the different depths showed similar trends over the course of the test.

5.3.9 Deflection in the Pavement Structure (Falling Weight Deflectometer)

Surface deflections measured with a falling weight deflectometer (FWD) on the untrafficked and trafficked areas of the section are summarized in Figure 5.15 (note that "trafficked area" and "untrafficked area" represent the FWD measurements taken on the HVS test section and adjacent to the HVS test section, respectively). Error bars represent the lowest and highest values. The results were consistent with the RSD measurements discussed previously, with the section exhibiting a small decrease in surface deflection of about 28 microns after completion of HVS trafficking. There was, however, a notable difference between the lowest and highest deflections along the section (444 microns), corresponding to the deeper rut and associated damage at one end of the section. A slight decrease in deflection was also noted in the untrafficked area, which was attributed in part to aging of the RHMA-G layer over the duration of the test, and in part to continued curing of the recycled layer. Note that FWD deflections are typically lower than RSD deflections because of the difference in the loading rate and testing temperatures (i.e., FWD measures deflection at simulated highway traffic speeds over a range of temperatures, whereas RSD deflection is measured at creep speeds at a single high temperature).

The recycled layer stiffness was backcalculated from the deflection measurements using the *CalBack* software package, and the results are summarized in Figure 5.16. Error bars represent the lowest and highest values. The average backcalculated stiffness of the RHMA-G layer (2,770 MPa) at the start of testing was lower than those of RHMA-G layers tested in previous projects (around 4,300 MPa). Average stiffness increased (about 590 MPa) after HVS trafficking, with a notable difference along the length of the section (1,200 MPa to 5,400 MPa), confirming the damage at the one end. The average stiffness of the untrafficked areas at either end of the test section also increased, consistent with the deflection measurements.

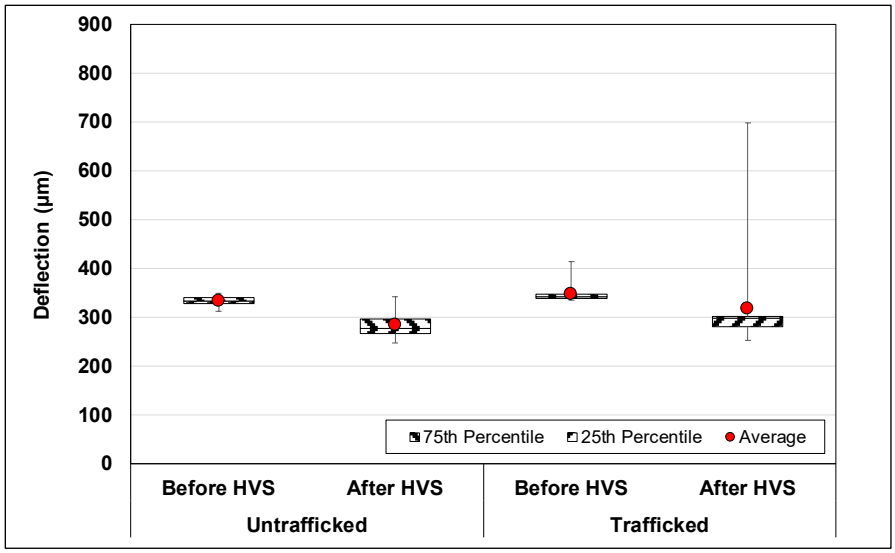

Figure 5.15: 704HB: Surface deflection (FWD).

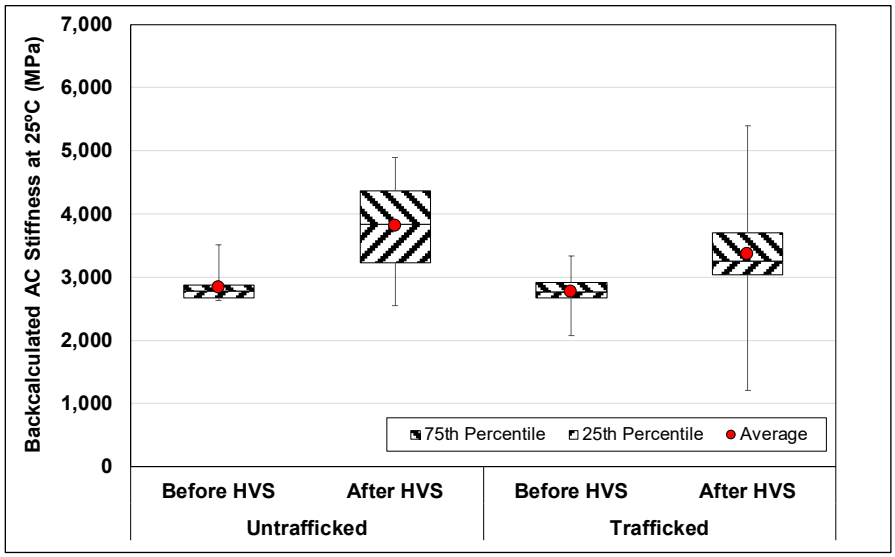

Figure 5.16: 704HB: Backcalculated stiffness of the RHMA-G layer (FWD).

5.3.10 Visual Assessment and Preliminary Forensic Coring

Apart from rutting, no other distresses were recorded on the test section. Photographs of the test section after HVS testing are shown in Figure 5.17 through Figure 5.20.

Cores were taken from the wheelpath at Station 13 and from the adjacent untrafficked area 600 mm (≈24 in.) from the outside edge of the wheelpath (Figure 5.21 and Figure 5.22, respectively). No distresses or debonding were noted on the cores. Thickness and air-void content measurements for the RHMA-G layer (Table 5.2) were measured on both cores and indicate that although there was no difference in air-void content between the wheelpath and

the untrafficked area, approximately 5.5 mm (0.21 in.) of rutting/densification was recorded in the wheelpath, confirming the observations from the MDD results.

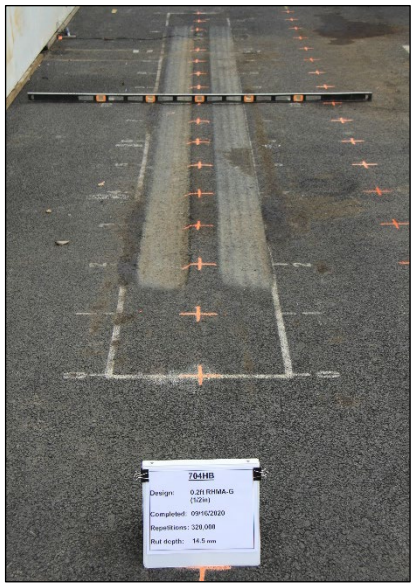

Figure 5.17: 704HB: Test section view from Station 0.

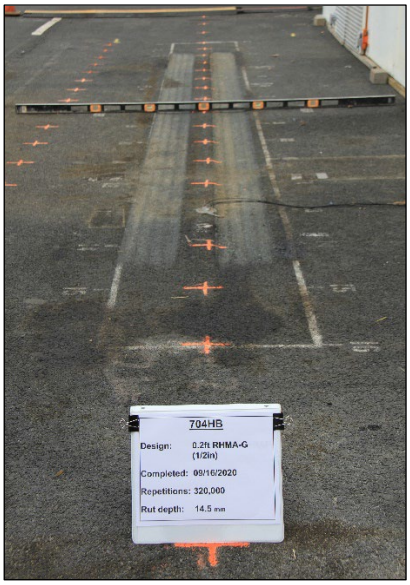

Figure 5.18: 704HB: Test section view from Station 16.

Figure 5.19: 704HB: View of rut at Station 8.

Figure 5.20: 704HB: Close-up view of surface at Station 8.

Figure 5.21: 704HB: Core taken in wheelpath.

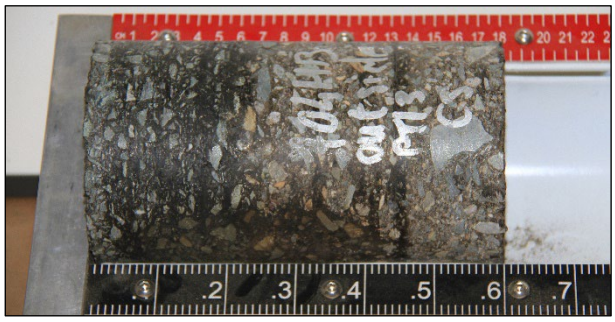

Figure 5.22: 704HB: Core taken 600 mm from edge of wheelpath.

Table 5.2: 704HB: Thickness and Air-Void Content Measurements from Cores

Property	Wheelpath	Untrafficked	Difference
RHMA-G thickness (mm [in.])	55.3 [2.18]	60.8 [2.39]	5.5 [0.21]
RHMA-G air-void content (%)	4.7	4.6	0.1

5.4 Section 701HC: 0.2 ft. RHMA-G (1/2 in.) with RAP

5.4.1 Test Summary

Loading commenced with a 40 kN half-axle load on September 23, 2019, and ended with an 80 kN load on July 23, 2020. A total of 300,000 load repetitions were applied and 39 datasets were collected. Load was increased from 40 kN to 60 kN after 160,000 load repetitions, and then to 80 kN after 260,000 load repetitions. The HVS loading history for Section 701HC is shown in Figure 5.23. Trafficking on this section was severely impacted, first because of a three-month breakdown resulting from a major hydraulic system failure, followed by a mandated four-month COVID-19 shutdown. It is not clear if this extended shutdown, coupled with a hydraulic oil spill, influenced the performance of the section. The test will be repeated on a new section if deemed appropriate based on an analysis of the data collected from the tests on all seven sections.

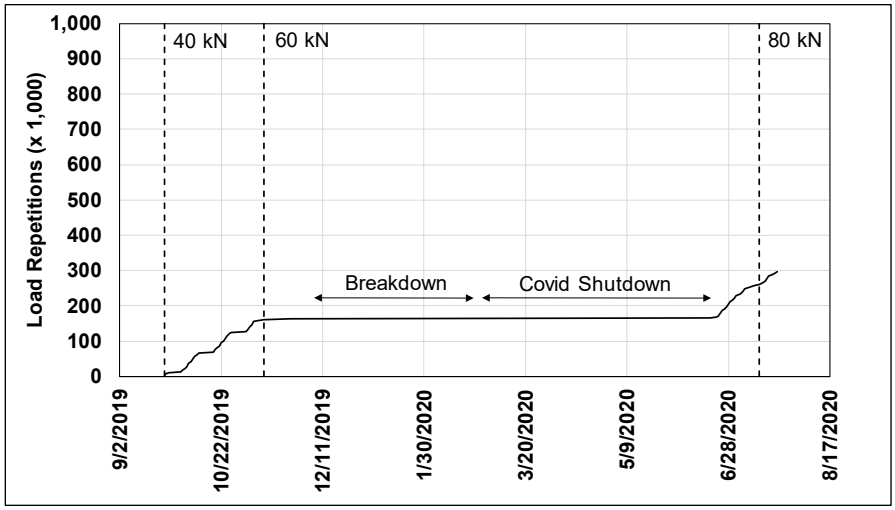

Figure 5.23: 701HC: HVS loading history.

5.4.2 Air Temperatures

Outside Air Temperatures

Daily 24-hour average outside air temperatures, measured with thermocouples attached to either side of the HVS environmental chamber (i.e., in direct sunlight), are summarized in Figure 5.24. Vertical error bars on each point on the graph show the daily temperature range.

Temperatures ranged from 5.9°C to 49.7°C (≈43°F to 121°F) during the course of HVS testing, with a daily 24-hour average of 25.8°C (≈78°F), an average minimum of 18.7°C (≈66°F), and an average maximum of 37.2°C (≈99°F).

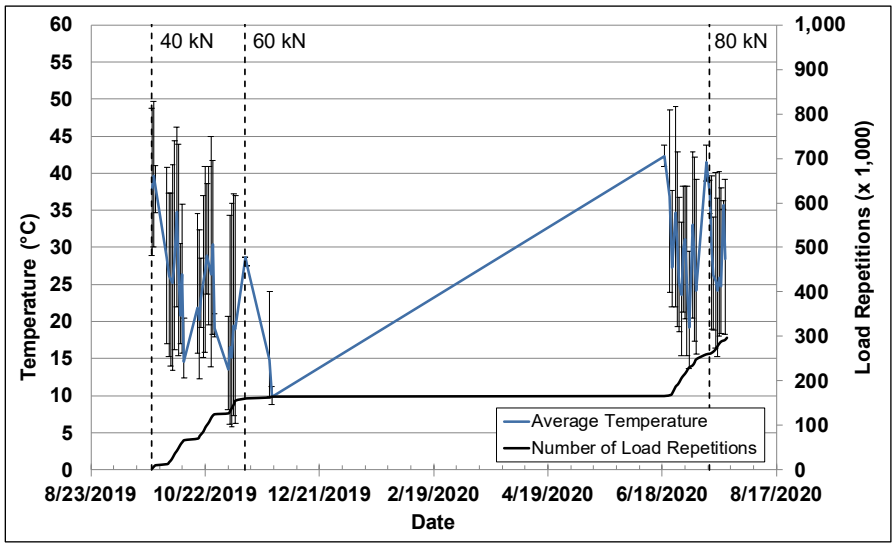

Figure 5.24: 701HC: Daily average air temperatures outside the environmental chamber.

Air Temperatures Inside the Environmental Chamber

The daily 24-hour average air temperatures, measured with thermocouples attached to either side of the HVS environmental chamber above the heaters and calculated from the hourly temperatures recorded during HVS operations, are shown in Figure 5.25. Vertical error bars on each point on the graph show the daily temperature range. During the test, air temperatures inside the environmental chamber ranged from 21.0°C to 52.0°C (≈70°F to 126°F) with an average of 38.1°C (≈100.6°F) and a standard deviation of 5.7°C (≈10.3°F). Air temperature was automatically adjusted with heater settings to maintain a pavement temperature of 50±2°C at a pavement depth of 50 mm. The recorded pavement temperatures discussed in Section 5.4.3 indicate that the inside air temperatures were adjusted appropriately to maintain the required pavement temperature.

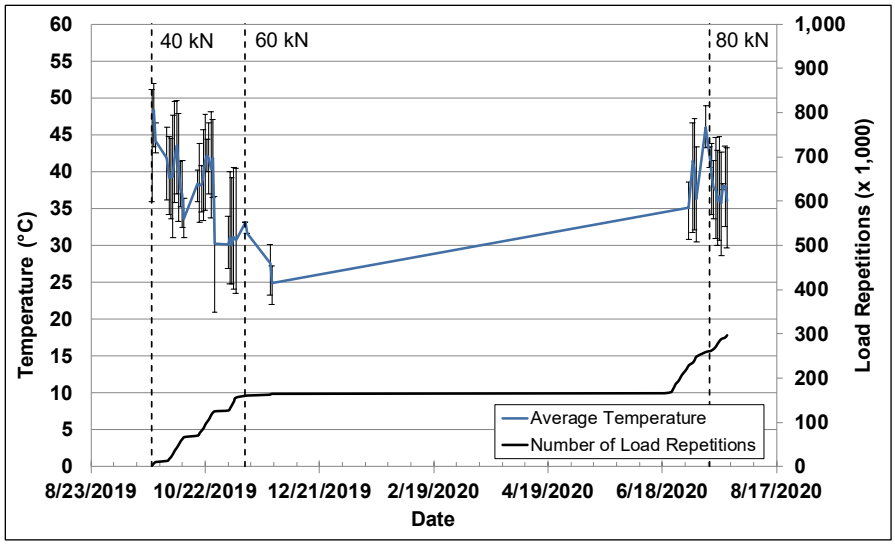

Figure 5.25: 701HC: Daily average air temperatures inside the environmental chamber.

5.4.3 Pavement Temperatures

Daily 24-hour averages of the air, surface, and in-depth temperatures of the RHMA-G and recycled layers are shown in Figure 5.26 and listed in Table 5.3. Pavement temperatures were constant and in the target range (50±2°C at a pavement depth of 50 mm) in the RHMA-G layer. Temperatures decreased with increasing depth in the underlying layers, as expected.

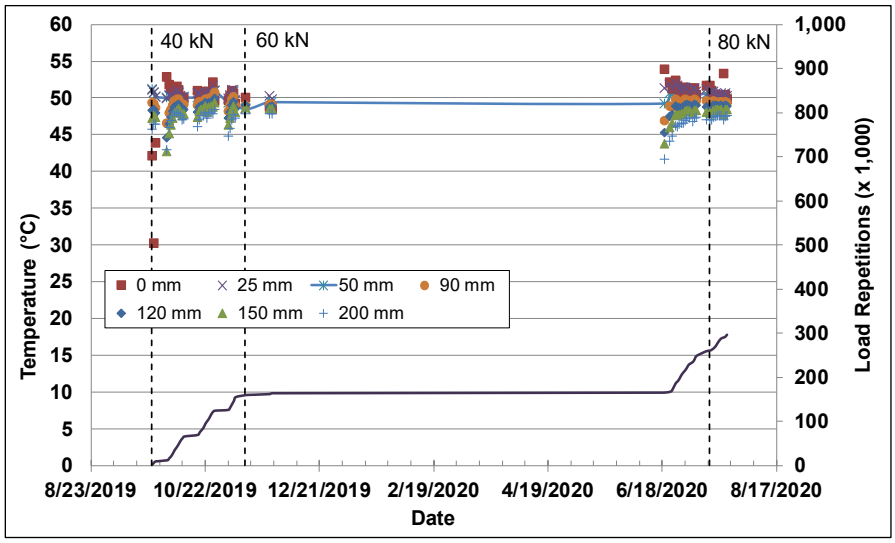

Figure 5.26: 701HC: Daily average pavement temperatures.

5.4.4 Permanent Deformation on the Surface (Rutting)

Figure 5.27 shows the average transverse cross section measured with the laser profilometer at various stages of the test. This plot clearly shows the initial high rate of rutting and increase in

rutting and deformation over time and that most of the deformation was in the form of a depression (i.e., deformation was below the zero elevation point at the surface [see Figure 4.5]). Minor upward and outward displacement of the material above the zero elevation point occurred during the last approximately 20,000 load repetitions after the load increase to 80 kN.

Table 5.3: 701HC: Summary of Air and Pavement Temperatures

Thermocouple Location	Layer	Temperature			
		Average (°C)	Std. Dev. (°C)	Average (°F)	Std. Dev. (°F)
Outside air	N/A	25.7	9.4	78.2	16.9
Inside air	N/A	38.1	5.7	100.6	10.3
Pavement surface	RHMA-G	50.1	6.4	122.2	11.4
25 mm below surface	RHMA-G	50.7	1.3	123.3	2.4
50 mm below surface	RHMA-G	50.4	0.9	122.7	1.6
90 mm below surface	Recycled	49.4	0.9	121.0	1.5
120 mm below surface	Recycled	48.7	0.9	119.6	1.7
150 mm below surface	Recycled	48.0	1.1	118.3	2.0
200 mm below surface	Aggregate base	47.1	1.2	116.8	2.2

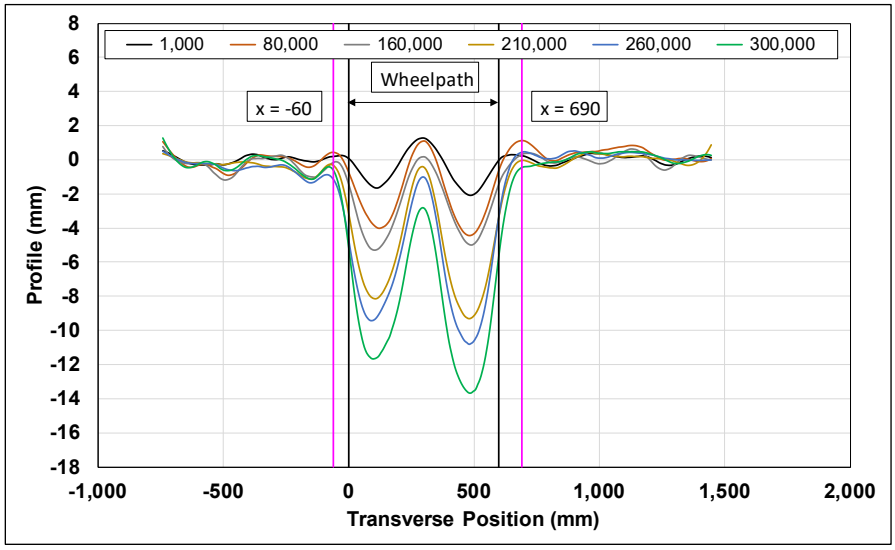

Figure 5.27: 701HC: Profilometer cross section at various load repetitions.

Figure 5.28 shows the development of permanent deformation (average maximum total rut and average deformation) with load repetitions. Error bars on the average maximum total rut indicate lowest and highest measurements along the section. These error bars indicate some variation along the section but less than that measured on Section 704HB. The embedment phase in this test occurred over a similar number of load repetitions to Section 704HB (i.e., ±20,000) but ended with a rut depth of about 4 mm (≈0.16 in.), considerably less than the 7 mm (≈0.28 in.) recorded

on Section 704HB. The reason for this difference is not clear, especially given that this section was tested before Section 704HB and was therefore subjected to less aging. However, the presence of the RAP may have stiffened the mix. The rate of increase of the rut depth after the embedment phase slowed considerably. The increase in the applied load to 60 kN resulted in a short embedment phase, followed by a steady rate of increase that was faster than that recorded during the 40 kN testing. This increase in rut rate may have been caused by the hydraulic oil spill. After the load increase to 80 kN, the rate of rut depth increased again and did not change significantly until the end of the test.

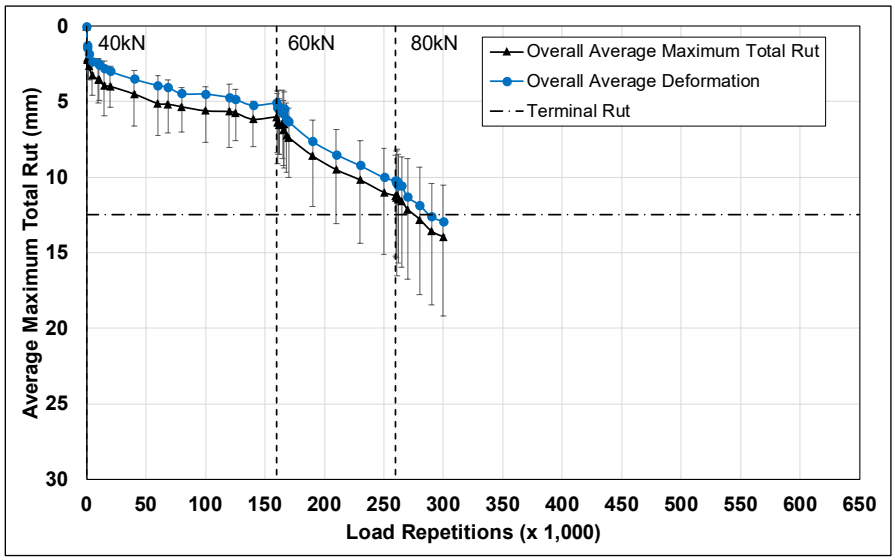

Figure 5.28: 701HC: Average maximum total rut and average deformation.

Figure 5.29 shows the average deformation and the deformation measured between Stations 3 and 7 and between Stations 8 and 13. Some variation along the length of the section was apparent, with higher levels of deformation between Stations 8 and 13 than between Stations 3 and 7. However, less variation was recorded on this test than on Section 704HB.

Figure 5.30 and Figure 5.31 show contour plots of the pavement surface at the start and end of the test (300,000 load repetitions). The end-of-test plot clearly shows the deeper rut at one end of the section.

Terminal rut (12.5 mm [≈0.5 in.]) was reached after approximately 285,000 load repetitions (≈1,077,000 ESALs). However, since the average maximum rut is calculated from measurements

at Stations 3 through 13, and the deeper rut at one end of the section influenced this average, trafficking was continued for another 15,000 additional load repetitions to further assess rutting trends at the 80 kN load.

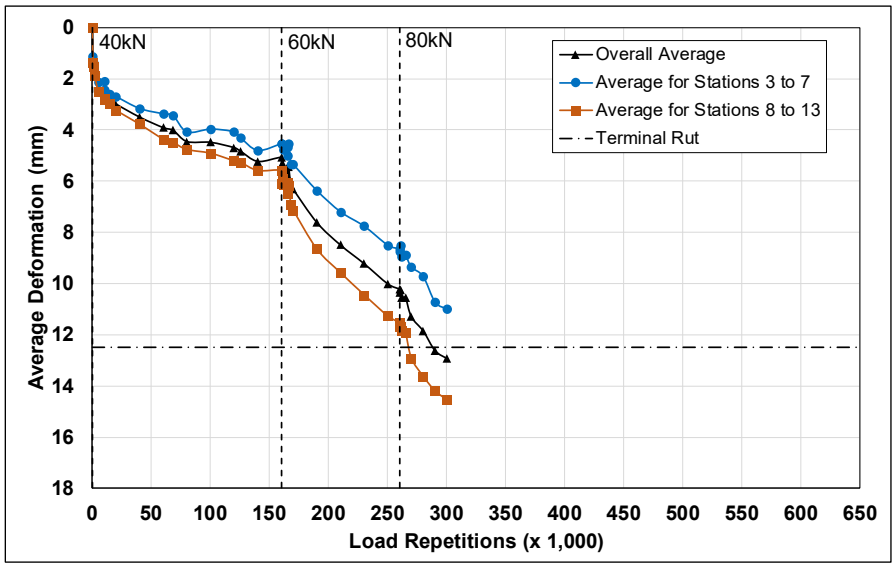

Figure 5.29: 701HC: Average deformation.

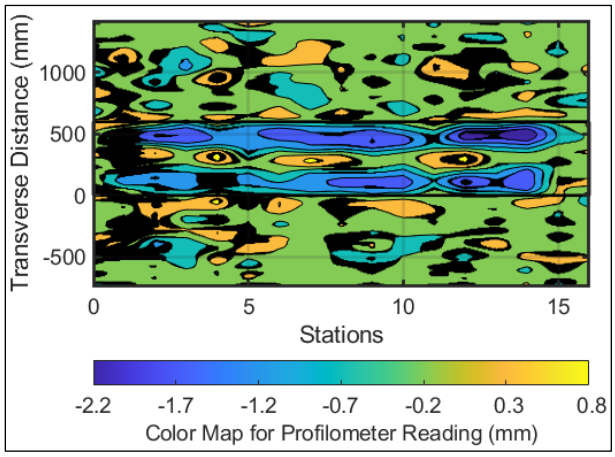

Figure 5.30: 701HC: Contour plot of permanent surface deformation at start of test.

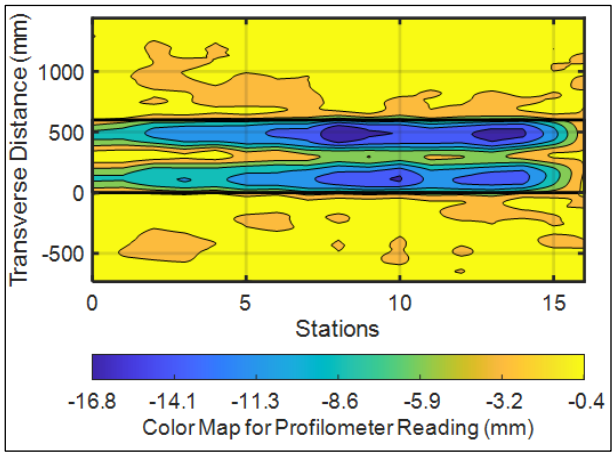

Figure 5.31: 701HC: Contour plot of permanent surface deformation at end of test.
(Note different scales in the legends.)

After completion of trafficking, the average maximum rut depth and the average deformation were 14.0 mm (≈0.55 in.) and 12.9 mm (≈0.51 in.), respectively. The maximum rut depth measured on the section was 16.9 mm (≈0.67 in.), recorded at Station 8.

5.4.5 Permanent Deformation in the Underlying Layers

Permanent deformation in the underlying layers, recorded with a multi-depth deflectometer (MDD) at Station 13 and compared to the surface layer (laser profilometer deformation [not total rut] measurement at Station 13), is shown in Figure 5.32. Note that the MDD measurements cannot be directly compared with those from the laser profilometer because the MDD was installed in the untrafficked area between the wheelpaths. This instrument location can therefore only provide an indication of which layer or layers the permanent deformation occurred in and not the actual deformation in each layer, which will be assessed during forensic investigations when all testing is completed.

Figure 5.32 shows that permanent deformation occurred primarily in the RHMA-G layer, with less in the CCPR and aggregate base layers. Minimal permanent deformation in the aggregate subbase and subgrade was recorded. There was a notable increase in permanent deformation in all of the layers after the load change to 60 kN.

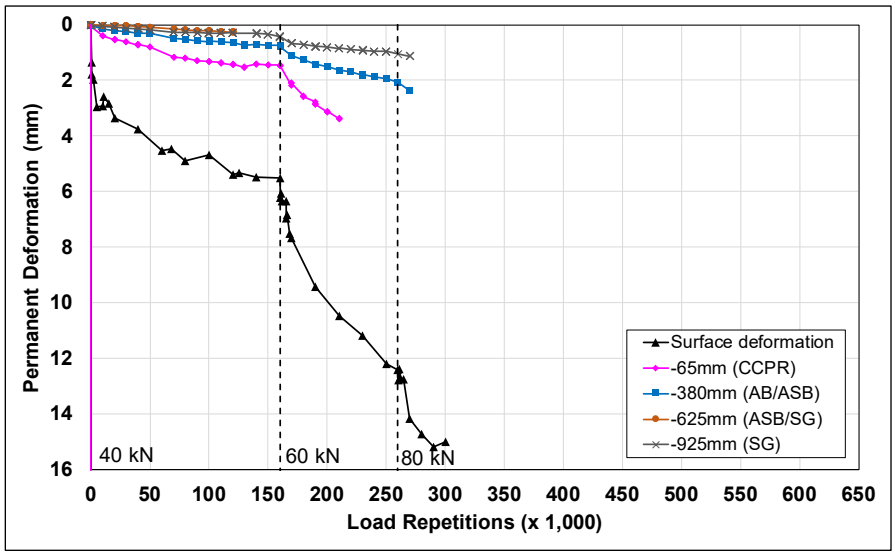

Figure 5.32: 701HC: Permanent deformation in the underlying layers.

5.4.6 Vertical Pressure at the Midpoint of the Aggregate Base Layer

Figure 5.33 shows the traffic-induced vertical pressure in the middle of the aggregate base layer. Note that vertical pressure measurements are recorded continuously during trafficking and spikes in the measurements indicate when manual measurements, which are done at creep wheel speed, were taken.

Vertical pressure readings were stable after some initial embedment, but sensitive to load change, for the duration of the test. Increases in recorded pressures occurred after the load changes, as expected. The results were consistent with those measured on Section 704HB.

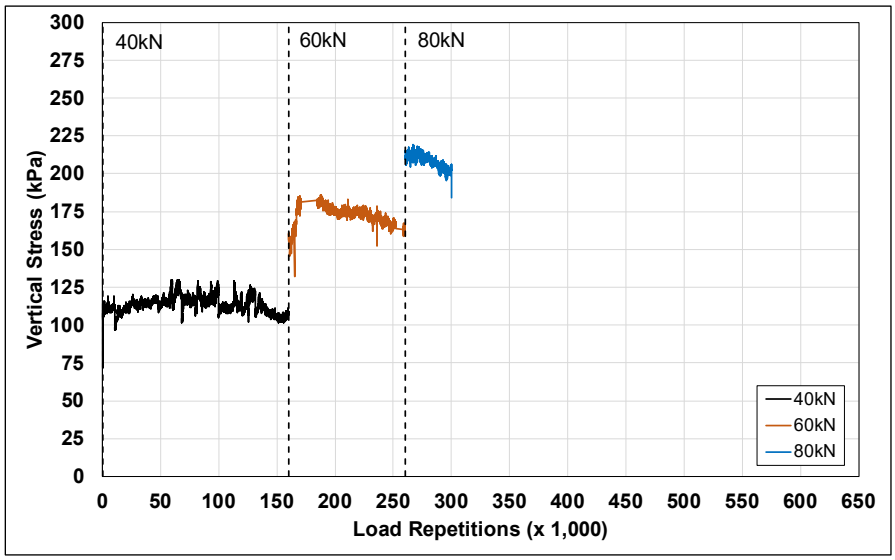

Figure 5.33: 701HC: Vertical pressure in the middle of the aggregate base layer.

5.4.7 Deflection on the Surface (Road Surface Deflectometer)

Figure 5.34 compares elastic surface deflections measured with a road surface deflectometer (RSD) under a 40 kN half-axle load. Deflections under the 60 kN and 80 kN loads are also shown. Deflections increased during the embedment phase of each load. Although deflections appeared to stabilize after the embedment phase under each load, deflection measured under the 40 kN load continued to increase, indicating that some permanent damage was occurring in the pavement under the 60 kN and 80 kN loads. Increases in absolute surface deflection were recorded on the section under the 60 kN and 80 kN loads, similar to those recorded on Section 704HB and as expected. Error bars on the plot indicate lowest and highest measurements along the section under a 40 kN load. These error bars indicate limited variability along the section during the 40 kN load testing but increases in variability at the higher wheel loads during the latter part of the test. This may be due to the hydraulic oil spill.

Deflections measured in the early part of the test under the 40 kN load were lower than those measured on the control section (704HB). This was attributed in part to early stiffening of the

mix resulting from blending of the recycled and virgin binders. Deflections in the latter part of the test were consistent with those measured on Section 704HB.

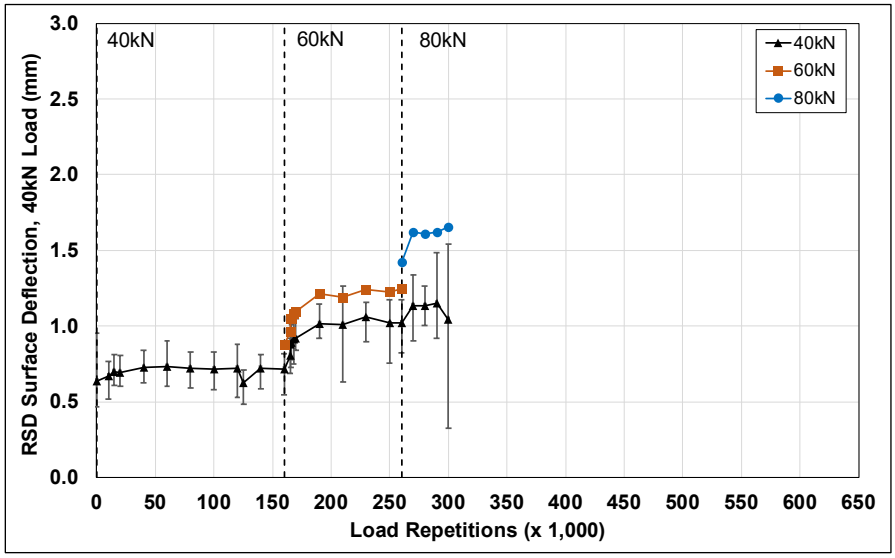

Figure 5.34: 701HC: Surface deflection (RSD).

5.4.8 Deflection in the Underlying Layers (Multi-Depth Deflectometer)

Figure 5.35 shows the history of in-depth elastic deflections measured by the LVDTs in the multi-depth deflectometer. These readings are consistent with the surface deflections measured with the RSD shown in Figure 5.34. Deflections in all layers remained stable for the duration of testing under a 40 kN wheel load. Deflections increased with increased load, as expected, and continued to increase at a very slow rate during trafficking, indicating that minimal damage was occurring under the heavier wheel loads. Deflection decreased with increasing depth, but the LVDTs at the different depths all showed similar trends over the course of the test.

5.4.9 Deflection in the Pavement Structure (Falling Weight Deflectometer)

Surface deflections measured with a falling weight deflectometer (FWD) on the untrafficked and trafficked areas of the section are summarized in Figure 5.36 ("trafficked area" and "untrafficked area" represent the FWD measurements taken on the HVS test section and adjacent to the HVS test section, respectively). Error bars represent the lowest and highest values. The results were consistent with the RSD measurements discussed above, with the section exhibiting a small increase in surface deflection of about 145 microns after completion of HVS trafficking, indicating that some damage occurred in the section during trafficking. No change in deflection was noted

in the untrafficked area. Note that FWD deflections are typically lower than RSD deflections because of the difference in the loading rate and testing temperatures (i.e., FWD measures deflection at simulated highway traffic speeds over a range of temperatures, whereas RSD deflection is measured at creep speeds at a single high temperature).

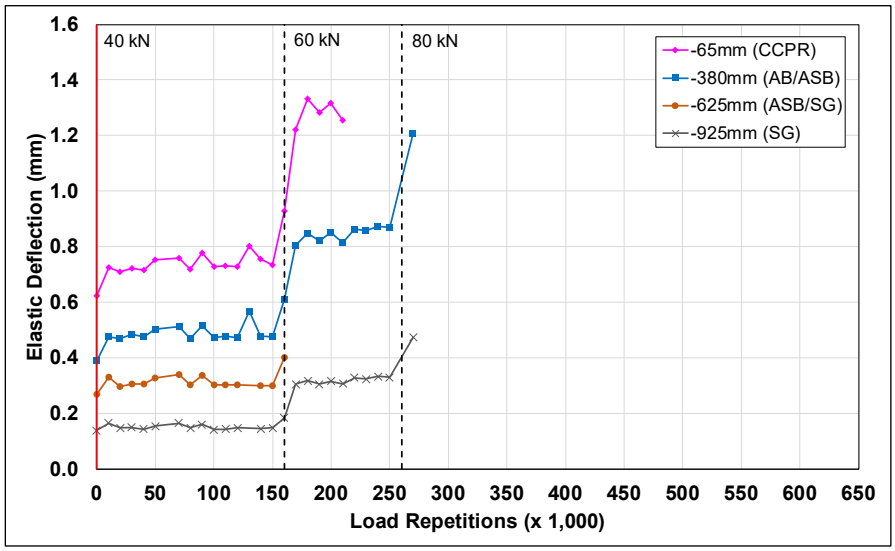

Figure 5.35: 701HC: Elastic deflection in the underlying layers.

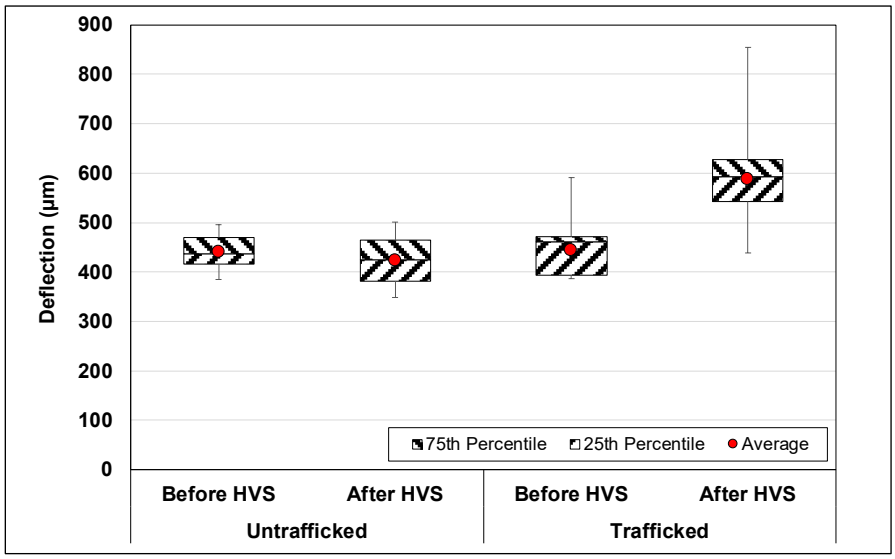

Figure 5.36: 701HC: Surface deflection (FWD).

The recycled layer stiffness was backcalculated from the deflection measurements using the *CalBack* software package and the results are summarized in Figure 5.37. Error bars represent the lowest and highest values. The average backcalculated stiffness of the RHMA-G layer (3,653 MPa) at the start of testing was marginally lower than that of RHMA-G layers tested in

previous projects (around 4,300 MPa) but marginally higher than that measured on Section 704HB. This was attributed in part to the presence of small amounts of stiffer reclaimed asphalt binder in the mix. Stiffness decreased by about 690 MPa during HVS trafficking, indicating that the trafficking and/or hydraulic oil spill did cause some damage in the RHMA-G layer. The stiffness of the untrafficked areas at either end of the test section also increased over the duration of the test (from 3,401 MPa to 4,076 MPa), further supporting the observation that small amounts of reclaimed asphalt binder had blended with the virgin binder over time. The untrafficked areas were not affected by the hydraulic oil leak.

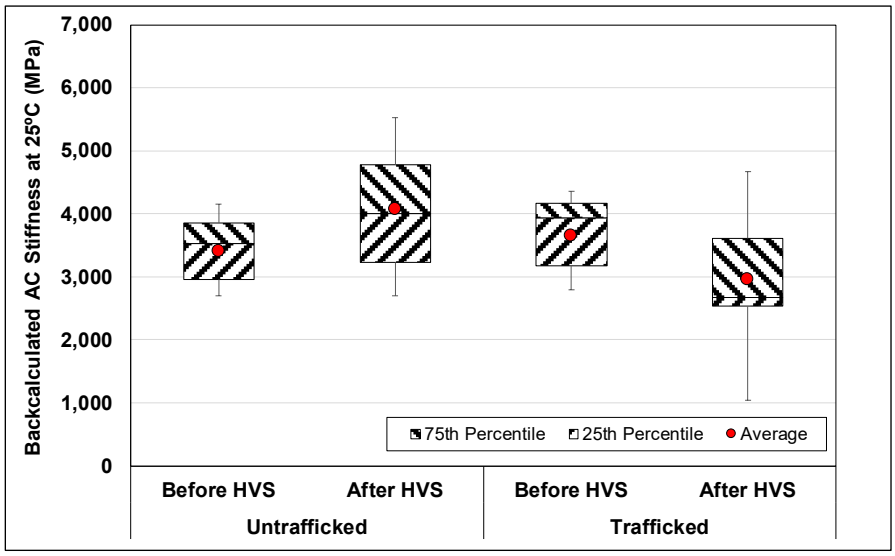

Figure 5.37: 701HC: Backcalculated stiffness of the RHMA-G layer (FWD).

5.4.10 Visual Assessment and Preliminary Forensic Coring

Apart from rutting, no other distresses were recorded on the section. Photographs of the test section after HVS testing are shown in Figure 5.38 through Figure 5.41.

Cores were taken from the wheelpath at Station 13 and from the adjacent untrafficked area 600 mm (≈24 in.) from the outside edge of the wheelpath (Figure 5.42 and Figure 5.43, respectively). No distresses or debonding were noted on the cores. Thickness and air-void content measurements for the RHMA-G layer (Table 5.4) were measured on both cores and indicate that although there was a small difference in air-void content between the wheelpath and the untrafficked area (0.8%), approximately 4.5 mm (0.18 in.) of rutting/densification was recorded in the wheelpath, confirming the observations from the MDD results.

Table 5.4: 701HC: Thickness and Air-Void Content Measurements from Cores

Property	Wheelpath	Untrafficked	Difference
RHMA-G thickness (mm [in.])	53.1 [2.09]	57.6 [2.27]	4.5 [0.18]
RHMA-G air-void content (%)	5.9	6.7	0.8

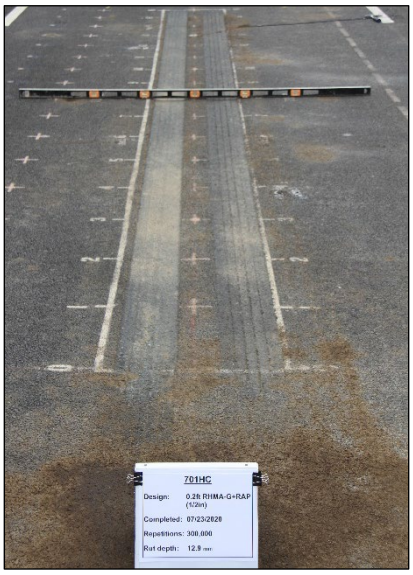

Figure 5.38: 701HC: Test section view from Station 0.

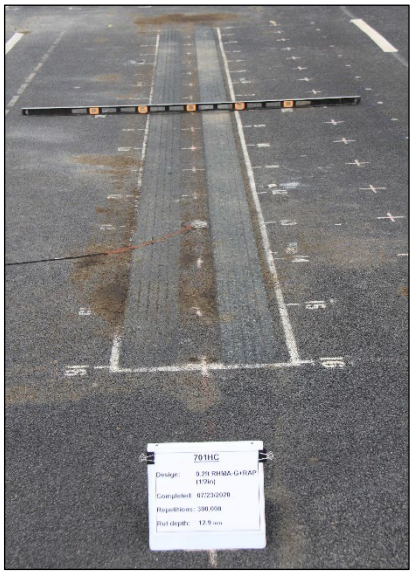

Figure 5.39: 701HC: Test section view from Station 16.

Figure 5.40: 701HC: View of rut at Station 8.

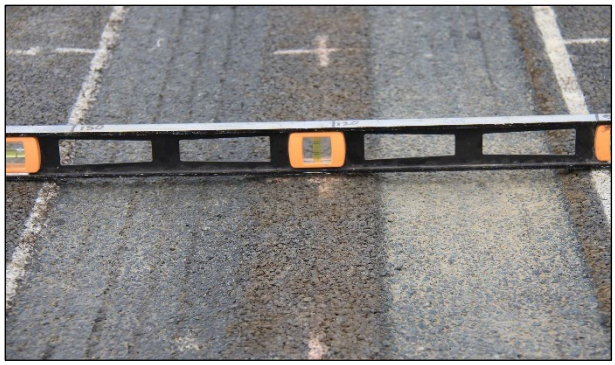

Figure 5.41: 701HC: Close-up view of test section surface at Station 8.

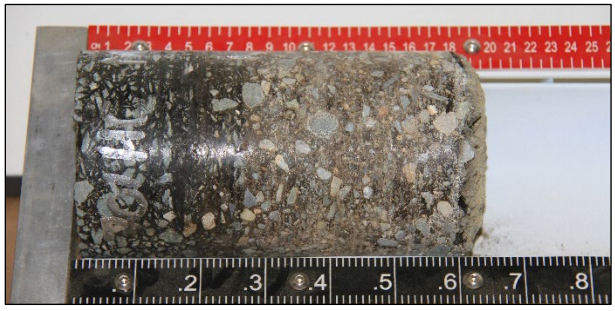

Figure 5.42: 701HC: Core taken in wheelpath.

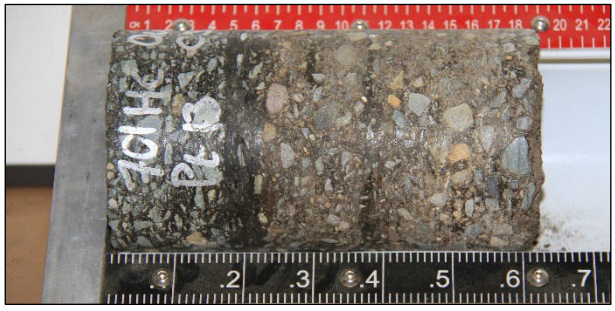

Figure 5.43: 701HC: Core taken 600 mm from edge of wheelpath.

5.5 Section 700HB: 0.5 ft. RHMA-G (3/4 in.) with RAP

5.5.1 Test Summary

Loading commenced with a 40 kN half-axle load on July 6, 2020, and ended with an 80 kN load on September 18, 2020. A total of 600,000 load repetitions were applied and 50 datasets were collected. Load was increased from 40 kN to 60 kN after 160,000 load repetitions and then to 80 kN after 260,000 load repetitions. The HVS loading history for Section 700HB is shown in Figure 5.44. A 15-day breakdown resulting from a hydraulic system failure occurred between August 25 and September 6 and a second 10-day breakdown resulting from an operating system failure occurred between September 26 and October 5.

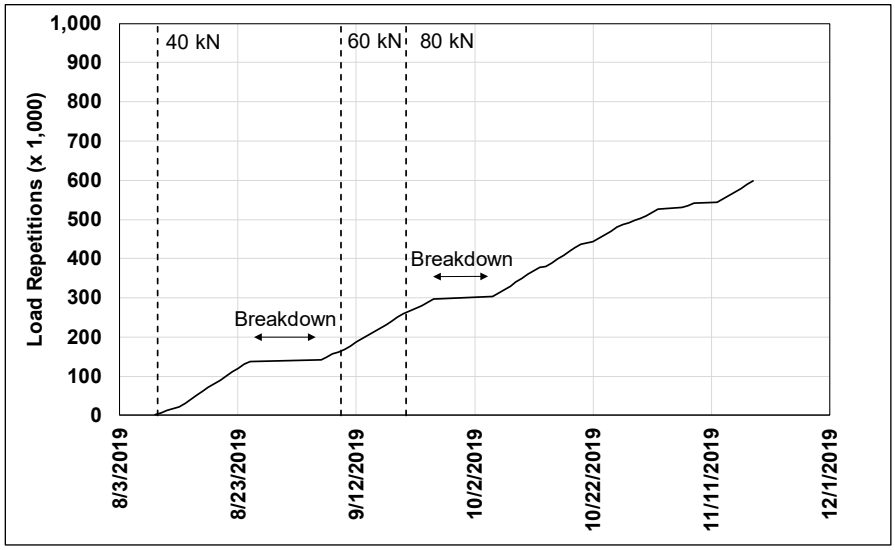

Figure 5.44: 700HB: HVS loading history.

5.5.2 Air Temperatures

Outside Air Temperatures

Daily 24-hour average outside air temperatures, measured with thermocouples attached to either side of the HVS environmental chamber (i.e., in direct sunlight), are summarized in Figure 5.45. Vertical error bars on each point on the graph show the daily temperature range. Temperatures ranged from 5.2°C to 50.3°C (≈41°F to 123°F) during the course of HVS testing, with a daily 24-hour average of 27.5°C (≈82°F), an average minimum of 18.5°C (≈65°F), and an average maximum of 38.4°C (≈101°F).

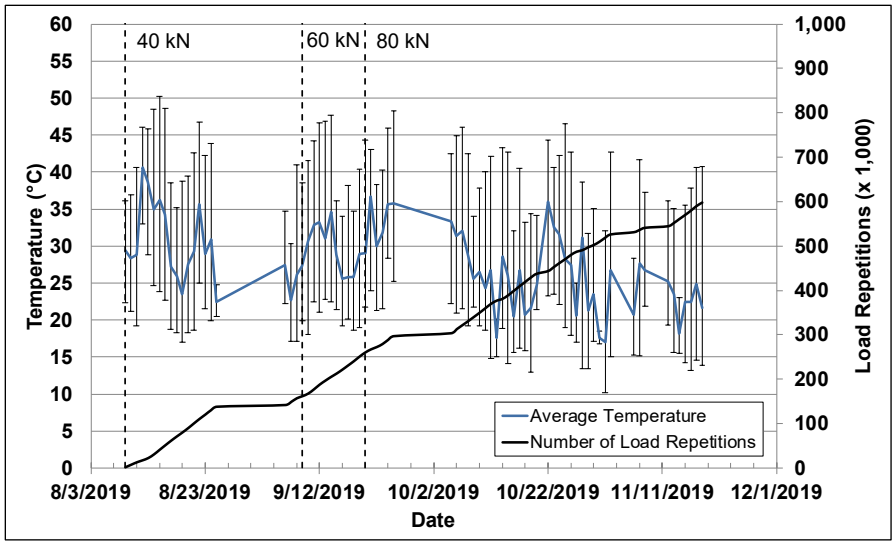

Figure 5.45: 700HB: Daily average air temperatures outside the environmental chamber.

Air Temperatures Inside the Environmental Chamber

The daily 24-hour average air temperatures, measured with thermocouples attached to either side of the HVS environmental chamber above the heaters and calculated from the hourly temperatures recorded during HVS operations, are shown in Figure 5.46. Vertical error bars on each point on the graph show the daily temperature range. During the test, air temperatures inside the environmental chamber ranged from 12.0°C to 52.0°C (≈54°F to 126°F) with an average of 43.5°C (≈110°F) and a standard deviation of 3.7°C (≈6.7°F). Air temperature was automatically adjusted with heater settings to maintain a pavement temperature of 50±2°C at a pavement depth of 50 mm (≈2.0 in.). The recorded pavement temperatures discussed in Section 5.5.3 indicate that the inside air temperatures were adjusted appropriately to maintain the required pavement temperature.

5.5.3 Pavement Temperatures

Daily 24-hour averages of the air, surface, and in-depth temperatures of the RHMA-G and recycled layers are shown in Figure 5.47 and listed in Table 5.5. Pavement temperatures were constant and in the target range (50±2°C at a pavement depth of 50 mm) in the RHMA-G layer. Temperatures decreased with increasing depth in the underlying layers, as expected.

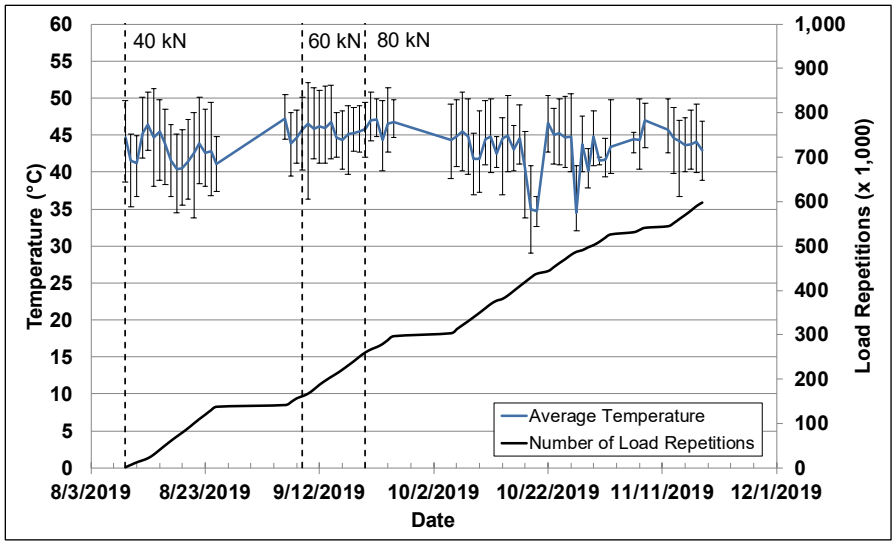

Figure 5.46: 700HB: Daily average air temperatures inside the environmental chamber.

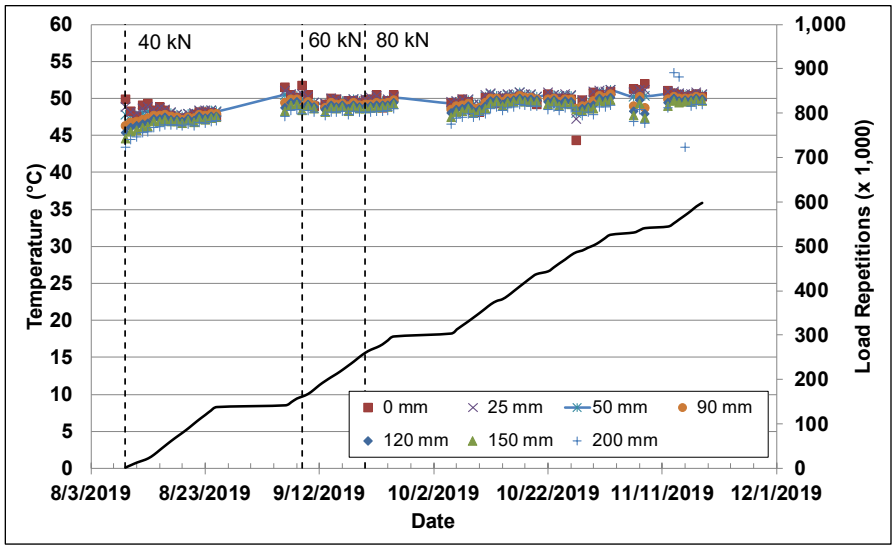

Figure 5.47: 700HB: Daily average pavement temperatures.

Table 5.5: 700HB: Summary of Air and Pavement Temperatures

Thermocouple Location	Layer	Temperature			
		Average (°C)	Std. Dev. (°C)	Average (°F)	Std. Dev. (°F)
Outside air	N/A	27.5	8.7	81.5	15.7
Inside air	N/A	43.5	3.7	110.3	6.7
Pavement surface	RHMA-G	49.3	3.0	120.7	5.5
25 mm below surface	RHMA-G	49.5	2.6	121.1	4.7
50 mm below surface	RHMA-G	49.3	2.6	120.8	4.7
90 mm below surface	RHMA-G	48.7	2.7	119.7	4.8
120 mm below surface	RHMA-G	48.4	2.7	119.0	4.9
150 mm below surface	RHMA-G	48.0	2.7	118.4	4.9
200 mm below surface	Recycled	47.4	3.9	117.4	7.1

5.5.4 Permanent Deformation on the Surface (Rutting)

Figure 5.48 shows the average transverse cross section measured with the laser profilometer at various stages of the test. This plot clearly shows the initial high rate of rutting and the increase in rutting and deformation over time and that most of the deformation was in the form of a depression (i.e., deformation was below the zero elevation point at the surface [see Figure 4.5]). Minor upward and outward displacement of the material above the zero elevation point occurred after the load increase to 60 kN.

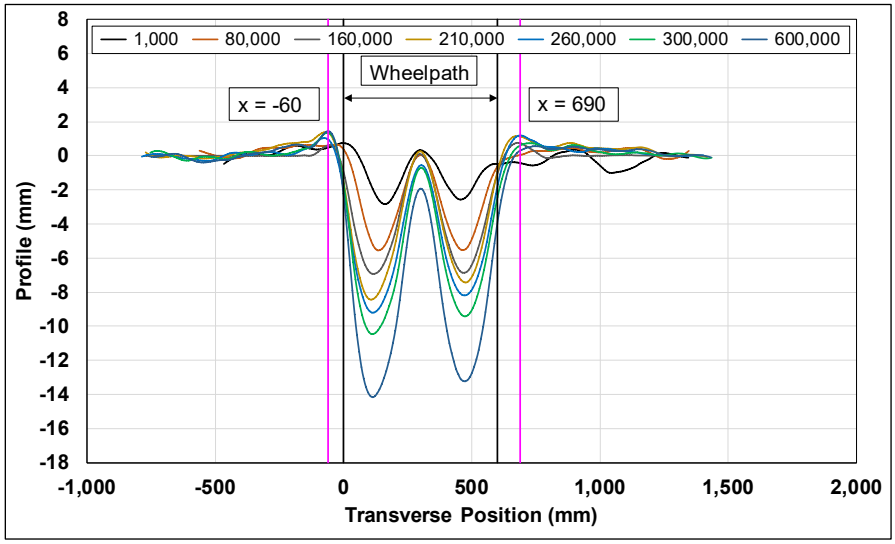

Figure 5.48: 700HB: Profilometer cross section at various load repetitions.

Figure 5.49 shows the development of permanent deformation (average maximum total rut and average deformation) with load repetitions. Error bars on the average maximum total rut line indicate lowest and highest measurement along the section. These error bars indicate some variation along the section but less than that measured on Section 704HB. The embedment phase in this test occurred over a similar number of load repetitions to Section 704HB (i.e., ±20,000), but ended with a rut depth of about 4 mm (≈0.16 in.), considerably less that the 7 mm (≈0.28 in.) recorded on Section 704HB. This was attributed in part to the thicker RHMA-G layers, the larger nominal maximum aggregate size, and/or the presence of RAP on this section.

The rate of increase of the rut depth after the embedment phase slowed considerably. Increases in the applied loads to 60 kN and 80 kN resulted in short embedment phases, before stabilizing to similar rates recorded during the 40 kN testing. This slower rut rate compared to Sections

704HB and 701HC was attributed primarily to the much thicker RHMA-G layers (150 mm [0.5 ft.] on this section compared to 60 mm [0.2 ft.] on the other two sections).

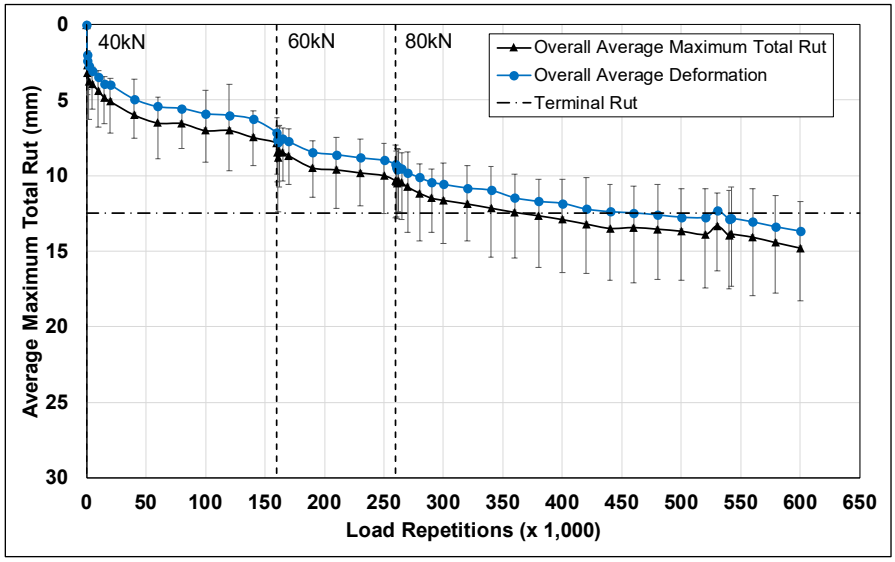

Figure 5.49: 700HB: Average maximum total rut and average deformation.

Figure 5.50 shows the average deformation and the deformation measured between Stations 3 and 7 and between Stations 8 and 13. Although the average rut depth was deeper between Stations 8 and 13, consistent with the other two tests, the difference between the rut depths on the two subsections was less than the other tests, indicating less variability along the length of the section.

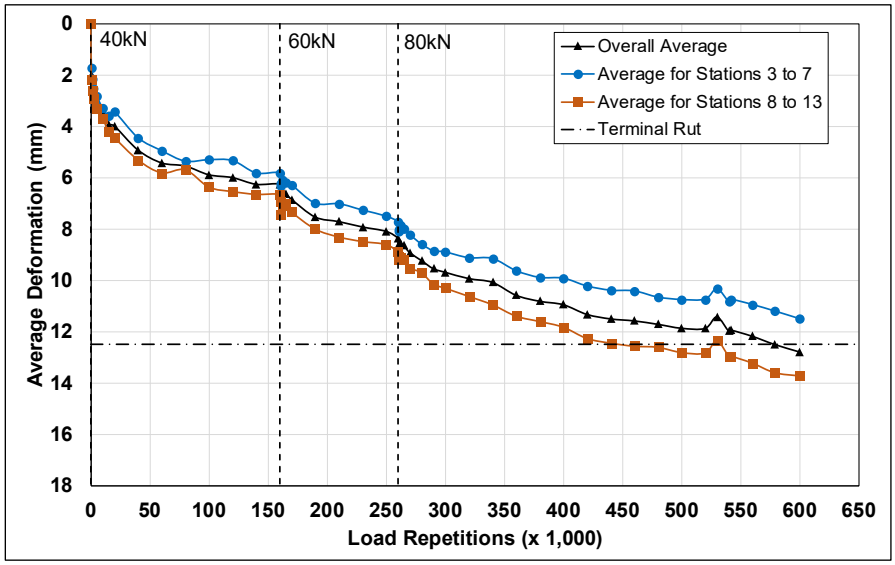

Figure 5.50: 700HB: Average deformation.

Figure 5.51 and Figure 5.52 show contour plots of the pavement surface at the start and end of the test (600,000 load repetitions). The end-of-test plot shows the deeper rut between Stations 8 and 13. Terminal rut (12.5 mm [≈0.5 in.]) was reached after approximately 370,000 load repetitions (≈2.73 million ESALs). However, since the average maximum rut is calculated from measurements at Stations 3 through 13, and the deeper rut at one end of the section influenced this average, trafficking was continued for another 230,000 additional load repetitions to further assess rutting trends at the 80 kN load. After completion of trafficking, the average maximum rut depth and the average deformation were 14.8 mm (≈0.58 in.) and 13.7 mm (≈0.54 in.), respectively. The maximum rut depth measured on the section was 15.8 mm (≈0.85 in.), recorded at Station 11.

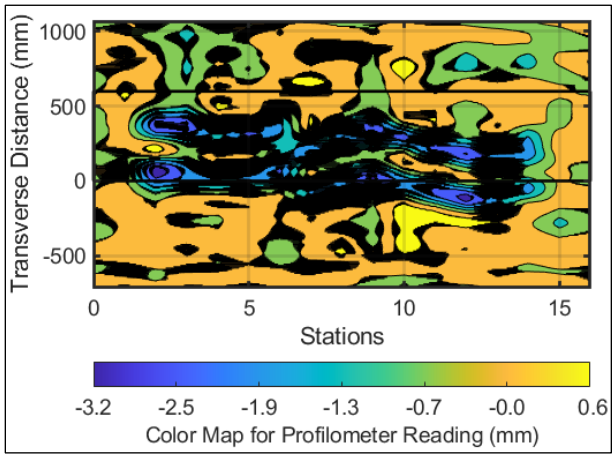

Figure 5.51: 700HB: Contour plot of permanent surface deformation at start of test.

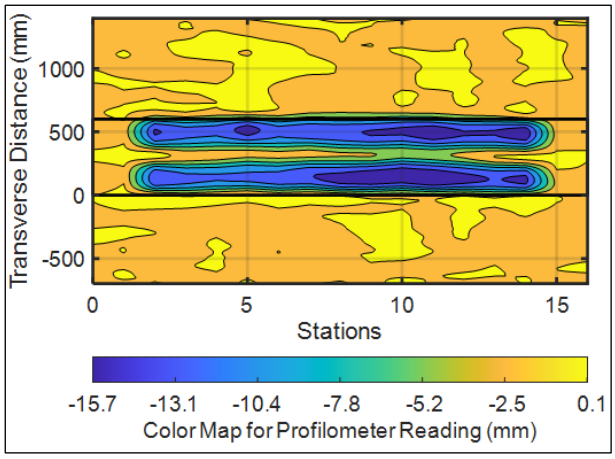

Figure 5.52: 700HB: Contour plot of permanent surface deformation at end of test.
(Note different scales in the legends.)

5.5.5 Permanent Deformation in the Underlying Layers

Permanent deformation in the underlying layers, recorded with a multi-depth deflectometer (MDD) at Station 13 and compared to the surface layer (laser profilometer deformation [not total rut] measurement at Station 13), is shown in Figure 5.53. The LVDTs appeared to have better survivability on this test compared to the tests on Sections 704HB and 701HC. Note that the MDD measurements cannot be directly compared with those from the laser profilometer because the MDD was installed in the untrafficked area between the wheelpaths. This instrument location can therefore only provide an indication of which layer or layers the permanent deformation

occurred in and not the actual deformation in each layer, which will be assessed during forensic investigations when all testing is completed.

Figure 5.53 shows that permanent deformation occurred primarily in the RHMA-G layer, consistent with the other two tests, with decreasing levels of permanent deformation in the CCPR, aggregate base, and aggregate subbase layers. Minimal permanent deformation was recorded in the subgrade. Notable increases in permanent deformation in the layers was not observed after the load changes, which was attributed to the thicker RHMA-G layer on this section.

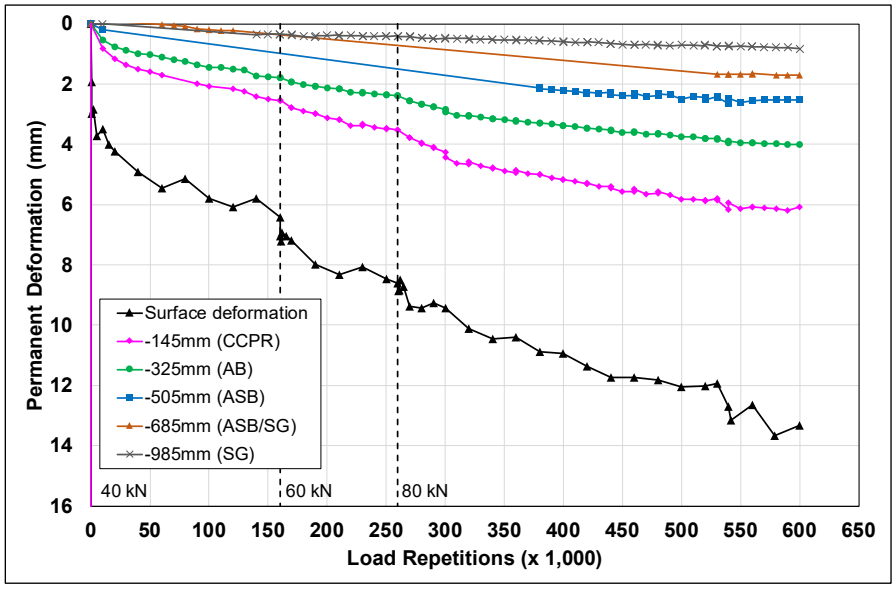

Figure 5.53: 700HB: Permanent deformation in the underlying layers.

5.5.6 Vertical Pressure at the Midpoint of the Aggregate Base Layer

Figure 5.54 shows the traffic-induced vertical pressure in the middle of the aggregate base layer. Note that vertical pressure measurements are recorded continuously during trafficking and spikes in the measurements indicate when manual measurements, which are done at creep wheel speed, were taken.

Vertical pressure readings were stable after some initial embedment, but sensitive to load change, for the duration of the test. Increases in recorded pressures occurred after the load changes, as expected. The results were consistent with those measured on Section 704HB.

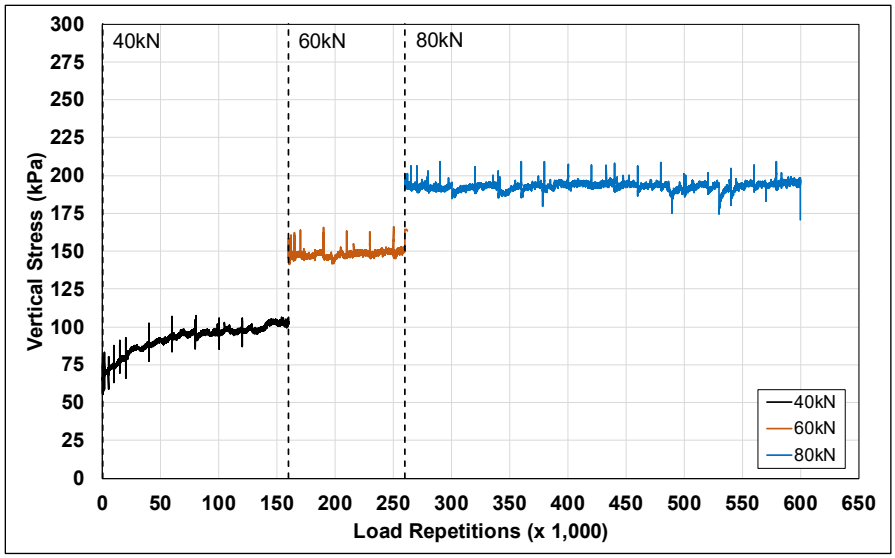

Figure 5.54: 700HB: Vertical pressure in the middle of the aggregate base layer.

5.5.7 Deflection on the Surface (Road Surface Deflectometer)

Figure 5.55 compares elastic surface deflections measured with a road surface deflectometer (RSD) under a 40 kN half-axle load. Deflections under the 60 kN and 80 kN loads are also shown.

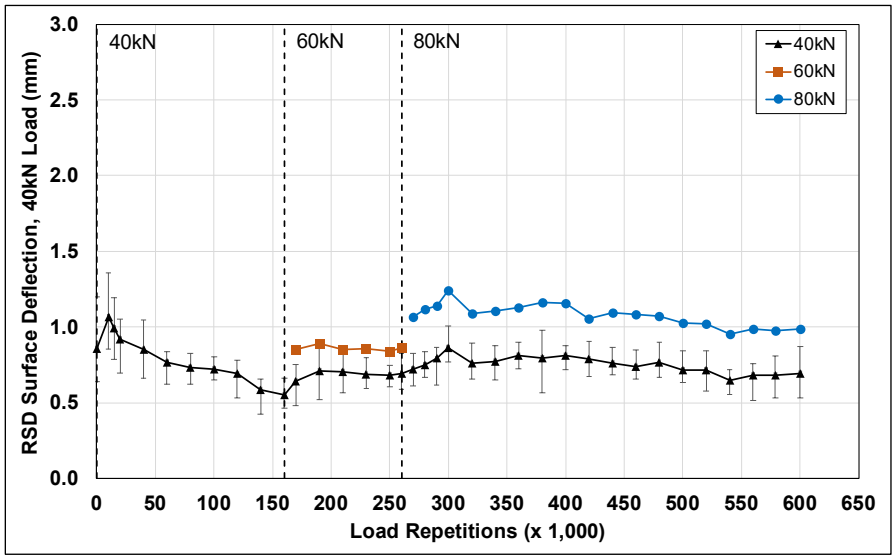

Figure 5.55: 700HB: Surface deflection (RSD).

Deflections increased during the embedment phase of each load. Although deflections appeared to stabilize after embedment under each load, deflection measured under the 40 kN load continued to increase, indicating that some permanent damage was occurring in the pavement under the 60 kN and 80 kN loads. Increases in absolute surface deflection were recorded on the

section under the 60 kN and 80 kN loads, as expected. Error bars on the plot indicate lowest and highest measurements along the section under the 40 kN load. These error bars indicate limited variability along the section during the 40 kN load testing but increases in variability at the higher wheel loads during the latter part of the test.

Deflections measured in the early part of the test under the 40 kN load were lower than those measured on the control section (704HB). This was attributed to the thicker RHMA-G layer. Deflections in the latter part of the test were consistent with those measured on Section 704HB.

5.5.8 Deflection in the Underlying Layers (Multi-Depth Deflectometer)

Figure 5.56 shows the history of in-depth elastic deflections measured by the LVDTs in the multi-depth deflectometer. These readings are consistent with the surface deflections measured with the RSD shown in Figure 5.55. Deflections decreased during the 40 kN wheel load trafficking suggesting some stiffening/densification in the layers attributable to HVS trafficking as well as the additional confinement provided by the thicker RHMA-G layer. Deflections increased with increased load, as expected, but then remained essentially the same for the duration of testing at that load, indicating that minimal damage was occurring in the underlying layers under the heavier wheel loads. Deflection decreased with increasing depth, but the LVDTs at the different depths all showed similar trends over the course of the test.

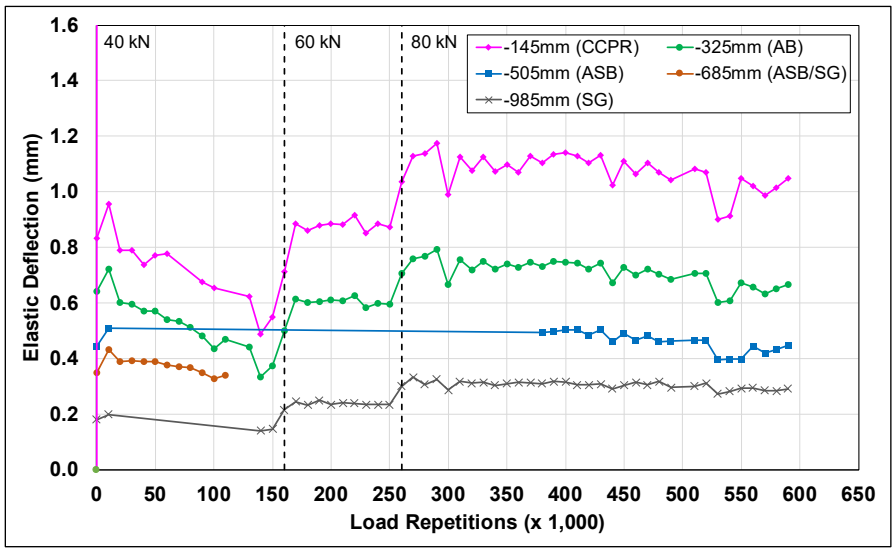

Figure 5.56: 700HB: Elastic deflection in the underlying layers.

5.5.9 Deflection in the Pavement Structure (Falling Weight Deflectometer)

Surface deflections measured with a falling weight deflectometer (FWD) on the untrafficked and trafficked areas of the section are summarized in Figure 5.57 ("trafficked area" and "untrafficked area" represent the FWD measurements taken on the HVS test section and adjacent to the HVS test section, respectively). Error bars represent the lowest and highest values. The results were consistent with the RSD measurements discussed above, with the section exhibiting a small decrease in surface deflection of about 135 microns after completion of HVS trafficking. This was attributed in part to blending of the aged reclaimed asphalt binder with the virgin asphalt rubber binder over time, given that a similar decrease in deflection was measured in the untrafficked area. Note that FWD deflections are typically lower than RSD deflections because of the difference in the loading rate and testing temperatures (i.e., FWD measures deflection at simulated highway traffic speeds over a range of temperatures, whereas RSD deflection is measured at creep speeds at a single high temperature).

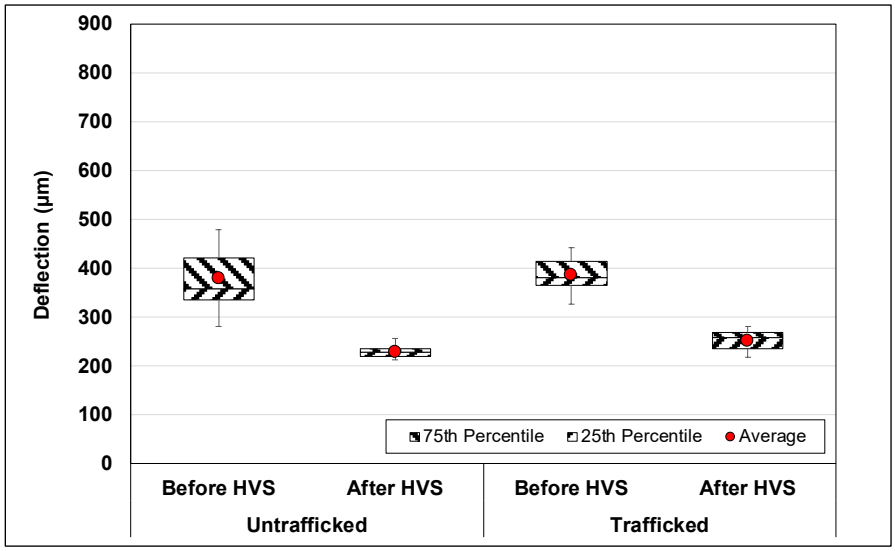

Figure 5.57: 700HB: Surface deflection (FWD).

The recycled layer stiffness was backcalculated from the deflection measurements using the *CalBack* software package and the results are summarized in Figure 5.58. Error bars represent the lowest and highest values. The average backcalculated stiffness of the RHMA-G layer (2,746 MPa) at the start of testing was considerably lower than those on RHMA-G layers tested in previous projects (around 4,300 MPa) and lower than those measured on Sections 704HB and 701HC. However, the average stiffness increased by about 1,630 MPa during HVS trafficking,

indicating that the trafficking did not cause any damage in the RHMA-G layer or that damage was masked by an increase in stiffness due to blending of the reclaimed asphalt and asphalt rubber binders over time. The stiffness of the untrafficked areas at either end of the test section also increased by a similar amount during the test (from 2,829 MPa to 4,621 MPa), further supporting the observation that some blending had occurred between the reclaimed and virgin asphalt binders.

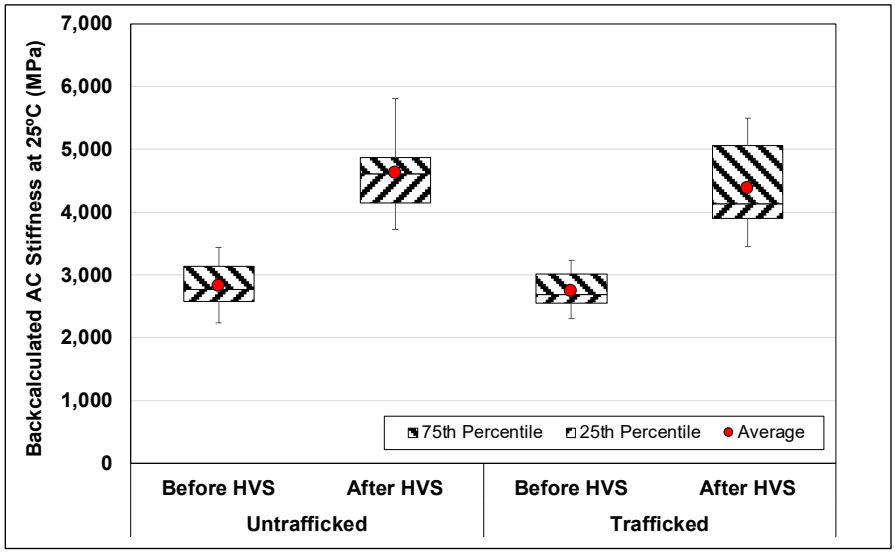

Figure 5.58: 700HB: Backcalculated stiffness of the RHMA-G layer (FWD).

5.5.10 Visual Assessment and Preliminary Forensic Coring

Apart from rutting, no other distress was recorded on the section. Photographs of the test section after HVS testing are shown in Figure 5.59 through Figure 5.62.

Cores were taken from the wheelpath at Station 13, and from the adjacent untrafficked area 600 mm (≈24 in.) from the outside edge of the wheelpath (Figure 5.63 and Figure 5.64, respectively). No distresses or debonding were noted on the cores. Thickness and air-void content measurements for the RHMA-G layers (Table 5.6) were measured on both cores, but some damage on the bottom lift of the core sampled from the untrafficked area caused during cutting prevented determination of an air-void content. In the top layers, the wheelpath air-void content was 1.8% lower than the untrafficked area and the core was 10.9 mm (0.43 in.) thinner, indicating that considerable rutting and densification had occurred in the top layer. The

difference in thickness between the bottom layers on the two cores was 1.7 mm (0.07 in.). These observations were consistent with the MDD results.

Table 5.6: 700HB: Thickness and Air-Void Content Measurements from Cores

Property	Layer	Wheelpath	Untrafficked	Difference
RHMA-G thickness (mm [in.])	Top	59.0 [2.32]	69.9 [2.75]	10.9 [0.43]
	Bottom	71.3 [2.81]	73.0 [2.87]	1.7 [0.07]
RHMA-G air-void content (%)	Top	3.8	5.6	1.8
	Bottom	3.3	Core damaged	N/A

Figure 5.59: 700HB: Test section view from Station 0.

Figure 5.60: 700HB: Test section view from Station 16.

Figure 5.61: 700HB: View of rut at Station 8.

Figure 5.62: 700HB: Close-up view of test section surface at Station 8.

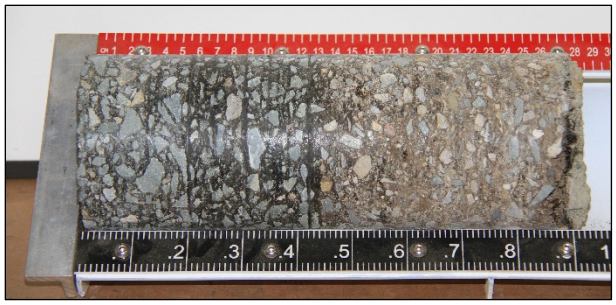

Figure 5.63: 700HB: Core taken in wheelpath.

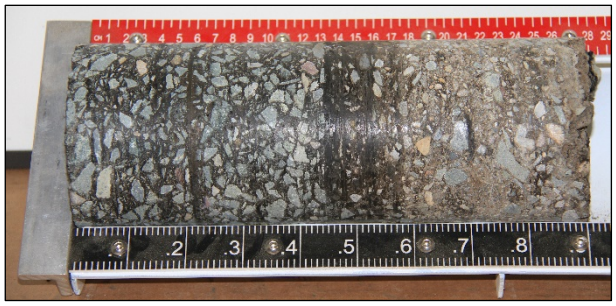

Figure 5.64: 700HB: Core taken 600 mm from edge of wheelpath.

5.6 Test Summary

The first three HVS tests discussed in this chapter covered the control section (0.2 ft. [60 mm], 1/2 in. with no RAP), a section with a single lift of 1/2 in. mix with RAP, and a section with two lifts of a 3/4 in. mix with RAP. Testing started in August 2019 and ended in September 2020. Testing was severely impacted by COVID-19 shutdown requirements, both in terms of HVS operations and in sourcing replacement parts to repair breakdowns to the hydraulic and load control systems.

A range of daily 24-hour average temperatures was experienced; however, pavement temperatures remained constant (50±2°C [≈122±4°F] at a pavement depth of 50 mm [≈2.0 in.]) throughout HVS trafficking.

Results from these first three HVS tests, which focused on rutting performance, indicate the following:

- Performance of all three mixes was satisfactory in terms of the level of trafficking required to reach a terminal average maximum rut of 12.5 mm (0.5 in.). The rate of rut depth development was slower on the test with two lifts of RHMA-G than on the two tests with single lifts of RHMA-G, as expected.
- The addition of RAP as a coarse aggregate replacement did not appear to have a significant influence on the test results.
- The backcalculated stiffnesses of the RHMA-G layer(s) on each section before and after HVS testing indicate that the trafficking did not cause any significant damage (i.e., loss in stiffness) in any of the three test sections. Stiffnesses increased after trafficking on two of the three sections, which was attributed to a combination of aging and densification of the layers under traffic. Some blending of reclaimed asphalt binder with the asphalt rubber

binder over time on these two sections, both containing RAP, may have contributed to this stiffness increase.

- No cracks were observed on any of the sections after trafficking.

Blank page

6. CONCLUSIONS

This technical memorandum summarizes a literature review update, elements of the construction of a test track to assess various aspects of gap-graded rubberized asphalt concrete (RHMA-G) mixes with and without the addition of reclaimed asphalt pavement (RAP) as aggregate replacement, and a first-level analysis of the results from the first three Heavy Vehicle Simulator (HVS) tests.

Apart from the research previously undertaken by the UCPRC for CalRecycle, only limited published research on the use of RAP in new RHMA mixes was located. The few documents available focused on laboratory testing of dense-graded mixes produced with terminal-blended binders containing completely digested rubber particles smaller than 0.4 mm (passing the #40 sieve). No documented research involving accelerated pavement testing of RHMA mixes containing RAP was located.

Four different RHMA-G mixes were placed on seven sections on the test track at the UCPRC. Mixes differed by nominal maximum aggregate size (NMAS; 1/2 and 3/4 in.) and the addition of 10% RAP by weight of the aggregate as a coarse aggregate replacement. Single and double lifts of each mix were placed. Apart from the addition of RAP, the mix designs all met current Caltrans specifications. Although Caltrans currently does not permit more than one lift of RHMA-G on projects, the placement of each lift of each mix on the test track met current Caltrans specifications for RHMA-G layers.

The first three HVS tests discussed in this technical memorandum covered the control section (0.2 ft. [60 mm], 1/2 in. NMAS with no RAP), a section with a single lift of 1/2 in. mix with RAP, and a section with two lifts of a 3/4 in. mix with RAP. Results from these first three HVS tests, which focused on rutting performance, indicated the following:

- Performance of all three mixes was satisfactory in terms of the level of trafficking required to reach a terminal average maximum rut of 0.5 in. (12.5 mm).
- The addition of RAP as a coarse aggregate replacement did not appear to have a significant influence on the test results.

- The backcalculated stiffnesses of the RHMA-G layer(s) on each section before and after HVS testing indicate that the trafficking did not cause any significant damage (i.e., loss in stiffness) in any of the three test sections. Stiffnesses increased after trafficking on two of the three sections, which was attributed to a combination of aging and densification of the layers under traffic. Some blending of reclaimed asphalt binder with the asphalt rubber binder over time on these two sections, both containing RAP, may have contributed to this stiffness increase.
- No cracks were observed on any of the sections after trafficking.

Given that only three sections have been tested to date, no recommendations on RHMA-G layer thicknesses or permitting the use of coarse RAP in RHMA-G mixes can be made at this time. These recommendations will be made after all the sections have been tested and the forensic investigations and associated laboratory testing have been completed.

REFERENCES

1. Alavi, Z., Hung, S., Jones, D. and Harvey, J. 2017. *Preliminary Investigation into the Use of Reclaimed Asphalt Pavement in Gap-Graded Asphalt Rubber Mixes, and Use of Reclaimed Asphalt Rubber Pavement in Conventional Asphalt Concrete Mixes.* Davis and Berkeley, CA: University of California Pavement Research Center. (UCPRC-RR-2016-03).
2. Xiao, F. 2006. *Development of Fatigue Predictive Models of Rubberized Asphalt Concrete (RAC) Containing Reclaimed Asphalt Pavement (RAP) Mixtures*. PhD Thesis, Clemson University.
3. Xiao, F., Amirkhanian, S.N. and Juang, C.H. 2007. Rutting Resistance of Rubberized Asphalt Concrete Pavements Containing Reclaimed Asphalt Pavement Mixtures. *Journal of Materials in Civil Engineering*, 19(6). (pp. 475-483).
4. Xiao, F. and Amirkhanian, S.N. 2009. Artificial Neural Network Approach to Estimating Stiffness Behavior of Rubberized Asphalt Concrete Containing Reclaimed Asphalt Pavement. *ASCE Journal of Transportation Engineering*, Vol. 135(8). (pp. 580-589).
5. Xiao, F. and Amirkhanian, S.N. 2009. Laboratory Investigation of Moisture Damage in Rubberized Asphalt Mixtures Containing Reclaimed Asphalt Pavement. *International Journal of Pavement Engineering*, Vol. 10(5). (pp. 319-328).
6. Xiao, F. and Amirkhanian, S.N. 2010. Laboratory Investigation of Utilizing High Percentage of RAP in Rubberized Asphalt Mixture. *Materials and Structures*, 43(1-2). (pp. 223-233).
7. Xiao, F., Amirkhanian, S.N., Putman, B.J. and Juang, H. 2012. Feasibility of Superpave Gyratory Compaction of Rubberized Asphalt Concrete Mixtures Containing Reclaimed Asphalt Pavement. *Construction and Building Materials,* Vol. 27. (pp. 432-438).
8. Luo, Z., Xiao, F., Hu, S. and Yang, Y. 2013. Probabilistic Analysis of Fatigue Life of Rubberized Asphalt Concrete Mixtures Containing Reclaimed Asphalt Pavement. *Construction and Building Materials*, Vol. 41. (pp. 401-410).
9. Vahidi, S., Mogawer, W.S. and Booshehrian, A. 2014. Effects of GTR and Treated GTR on Asphalt Binder and High-RAP Mixtures. *Journal of Materials in Civil Engineering*, Vol 26(4). (pp 721-727).
10. Ambaiowei, D.C. and Tighe, S.L. 2015. Rubberized Asphalt Mixtures with RAP: A Case for Use in Ontario. *Proceedings 94th Transportation Research Board Annual Meeting*. Washington, DC: Transportation Research Board.
11. Jones, D. 2005. *Quality Management System for Site Establishment, Daily Operations, Instrumentation, Data Collection, and Data Storage for APT Experiments.* Pretoria, South Africa: CSIR Transportek. (Contract Report CR-2004/67-v2).

Blank page